Groundwater recharge estimation using in-situ and GRACE observations in the eastern region of the United Arab Emirates

Khaled Alghafli [a,b,*], Xiaogang Shi [c], William Sloan [a], Mohammad Shamsudduha [d], Qiuhong Tang [e], Ahmed Sefelnasr [b], Abdel Azim Ebraheem [b]

[a] *James Watt School of Engineering, University Glasgow, UK*
[b] *The National Water and Energy Center, United Arab Emirates University, Al Ain, United Arab Emirates*
[c] *School of Interdisciplinary Studies, University of Glasgow, Dumfries, UK*
[d] *Institute for Risk and Disaster Reduction, University College London, London, UK*
[e] *Key Laboratory of Water Cycle and Related Land Surface Processes, Institute of Geographic Sciences and Natural Resources Research, Chinese Academy of Sciences, Beijing, China*

HIGHLIGHTS

- GRACE is able to capture the massive groundwater depletion, resulting from the intensive agricultural practices from 2002 to 2011 in the UAE.
- The decomposed GRACE timeseries showed a better agreement with in-situ data than the seasonal trend.
- The downscaled 0.5° grids showed similar terrestrial water storage trend variation with the native 3-degree grid.
- GRACE for recharge estimation in the arid regions can be used to support the decision-making process.

GRAPHICAL ABSTRACT
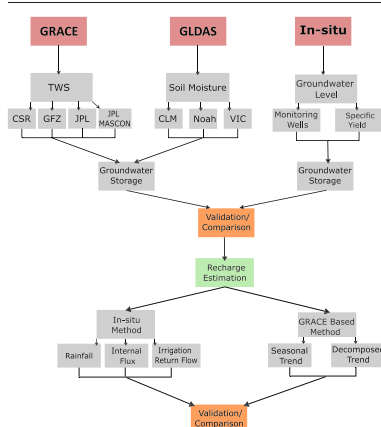
ARTICLE INFO

ABSTRACT

The intensive agricultural expansion and rapid urban development in Abu Dhabi Emirate, United Arab Emirates (UAE) have resulted in a major decline in local and regional groundwater levels. By using the latest release (RL06) of Gravity Recovery and Climate Experiment (GRACE) satellite measurements and Global Land Data Assimilation System (GLDAS) products, the groundwater storage change was computed and compared with the time series of in-situ monitoring wells over the period of 2010–2016. The RL06 GRACE products from Jet Propulsion Laboratory (JPL), University of Texas Center for Space Research (CSR), German Research Center for Geosciences (GFZ), and JPL mass concentrations (MASCON) were assessed and have shown satisfactory agreements with the monitoring wells. The JPL MASCON reflected the in-situ groundwater storage change better than the other GRACE products ($R = 0.5$, lag $=1$ month, RMSE $= 13$ mm). The groundwater recharge is estimated for the study area and compared with the in-situ recharge method that considers multi recharge components from the rainfall, irrigation return flow and internal fluxes. The results show that the agreements between in-situ and GRACE-derived recharge estimates are highly agreeable (e.g., $R^2 = 0.91$, RMSE $= 1.5$ Mm^3 to 7.8 Mm^3, and Nash-Sutcliff Efficiency $= 0.7$). Using the Mann-Kendall trend test and Sen's slope, the analyses of policies, number of wells, and farm areal expansion with groundwater time series derived from GRACE helped to validate GRACE and emphasize the importance of regulations for sustainable development of groundwater resources. The impacts of subsidy cuts after 2010 can be captured from the

GRACE data in the eastern region of Abu Dhabi Emirate. The linear trend of groundwater storage anomaly obtained from GRACE over the period from 2003 to 2010 is -6.36 ± 0.6 mm/year while it showed a decline trend of -1.2 ± 0.6 mm/year after the subsidy cut. The proposed approach has a potential application for estimating groundwater recharge in other arid regions where in-situ monitoring wells are limited or absent.

1. Introduction

Rapid economic development and high rates of population growth have increased the demand for freshwater resources globally (An et al., 2021; Abbott et al., 2019) and severely caused groundwater depletion in many aquifers with an alarming rate (Rateb et al., 2020; Long et al., 2016; Rodell et al., 2018; Madani et al., 2016; Alsharhan and Rizk, 2020a; Shamsudduha and Taylor, 2020). More than half of the of the annual freshwater consumption worldwide is sourced from groundwater resources for various purposes such as agriculture, industry, and domestic use (Margat and Van der Gun, 2013; Taylor et al., 2022). In arid and semi-arid regions, about 60 % of the exploited groundwater is nonrenewable (World-Bank, 2017) where millions of groundwater wells are vulnerable to dry if the groundwater level declines by few meters (Jasechko and Perrone, 2021). Therefore, the intense depletion of groundwater resources and the limited water availability attracted scientists to seek sustainable solutions to manage groundwater resources for arid regions (Davijani et al., 2016; Yu et al., 2019; Ghorbal et al., 2021).

The eastern region of Abu Dhabi Emirate, the United Arab Emirates (UAE) is in an arid region with minimal renewable freshwater resources. The unconfined surficial aquifer (known as Quaternary aquifer), is a transboundary aquifer shared between the UAE, Saudi Arabia, and Sultanate of Oman, and it is the major source of groundwater in this region. This aquifer is currently facing dramatic groundwater depletion and saltwater intrusion owing to overexploitation and the prevailing drought conditions (EAD, 2018). To reduce food imports in the UAE, the agriculture sector underwent a significant expansion in the eastern region of Abu Dhabi Emirate

during the 1990s, which caused several cones of depression in the Quaternary aquifer in the farm areas, as shown in Fig. 1. Consequently, the groundwater levels declined by >60 m relative to the steady state level in 1969 (Atlas, 2013; Alsharhan and Rizk, 2020b). According to the recent study by Sherif et al. (2021), the groundwater renewability in this region is only 40 % (i.e.,1.2 km³ out of the 3 km³ annual extraction rate). To preserve groundwater resources and set sustainable groundwater management policies, detailed knowledge of changes in groundwater storage and the condition of the aquifer system is required (Dennehy et al., 2015). However, the lack of groundwater data hinders water managers from quantitively evaluating the effectiveness of water management solutions (White et al., 2016).

Many studies were conducted on quantifying the changes in groundwater storage and simulating aquifer dynamics in the UAE. Sherif et al. (2018) used the potential recharge method which is based on an empirical method involving multiple parameters, to estimate the recharge component from rainwater percolation to the Quaternary aquifer in the UAE. However, the internal flux, an important recharge component in the eastern region, along the border with Oman, was not considered in their estimation. The wadi (valley) recharge near the basins in Oman Mountains travels through bedrock fractures towards the UAE border where it discharges into fan deposits or piedmonts (Woodward and Menges, 1992). By using the numerical runoff-infiltration model and water-balance model for 17 basins in Oman Mountains, the annual internal flow recharge in the Al Ain area from Oman Mountains was estimated to be approximately 55 Mm³ (Osterkamp et al., 1995). The United States Geological Survey (USGS) modelled the regional pre-development groundwater flow system in the
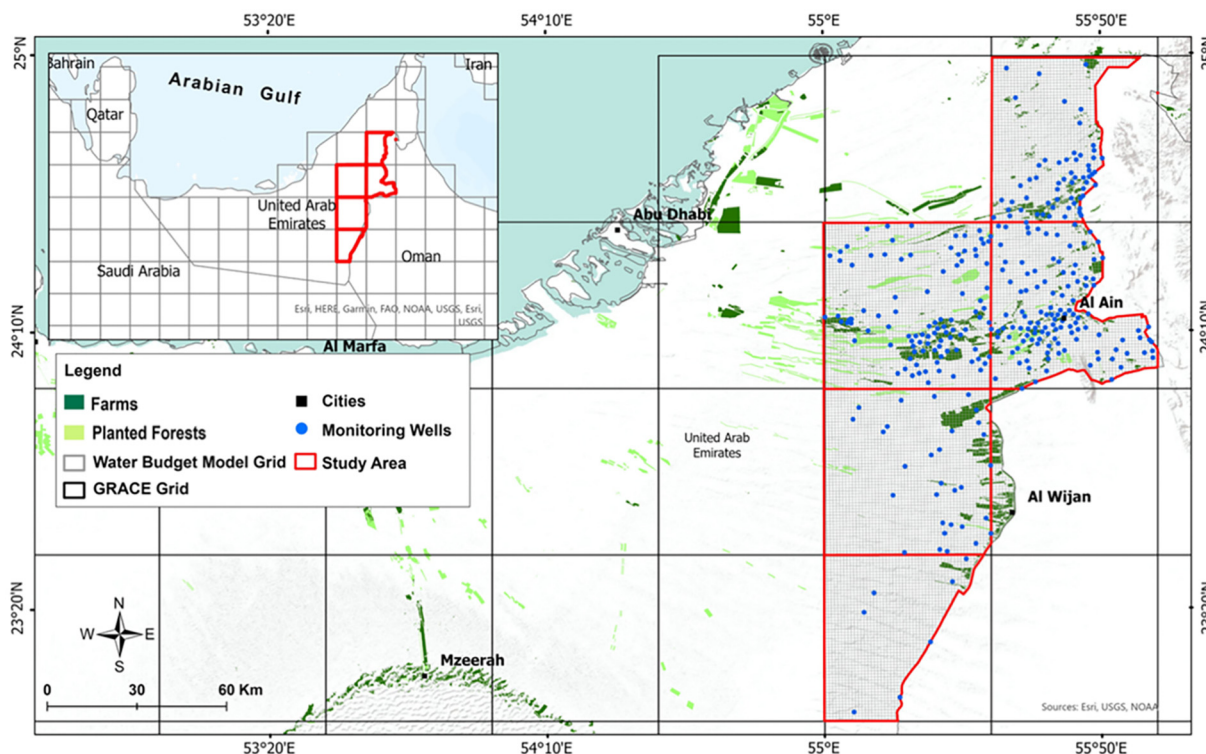

Fig. 1. The study area with monitoring wells, farms, planted forests, and GRACE grids.

eastern region of Abu Dhabi Emirate and applied different recharge model scenarios for model assessments (Eggleston et al., 2018), and obtained a similar internal flow recharge rate. Sathish et al. (2018) developed a groundwater flow model for the Quaternary aquifer in Abu Dhabi Emirate and their results indicated that subsurface groundwater flow from Oman mountains was the largest recharge contributor. Sherif et al. (2021) developed a water budget model using a statistical approach to estimate the changes in groundwater storage in the Quaternary aquifer. These different approaches improved our understanding of the groundwater resources of Quaternary aquifer in the UAE.

The integration of in-situ data with remote sensing data can help on expanding the knowledge of hydrological cycle (Rodell et al., 2015). The Gravity Recovery and Climate Experiment (GRACE) satellites, launched in 2002, have provided an alternative solution to estimate terrestrial water storage (TWS) (Tapley et al., 2004). The GRACE mission is to calculate the TWS components including groundwater storage, surface water storage, soil moisture storage, and snow water storage (Rodell and Famiglietti, 2001; Tapley et al., 2004; Shamsudduha et al., 2012). The subtraction of other TWS components from GRACE can result in an anomaly that represents groundwater storage. Those TWS components (e.g., soil moisture, surface water and, snow water) can be estimated using the land surface models (LSMs) run by the NASA's Global Land Data Assimilation System (GLDAS).

Generally, quantifying groundwater recharge requires to collect in-situ data with a detailed knowledge of field hydrologic parameters (Chen et al., 2016; Fu et al., 2019) and anthropogenic practices (Han et al., 2017). However, there is no study in the UAE that incorporated the NASA's GRACE satellites data with in-situ hydrogeological analysis to quantify groundwater recharge of the Quaternary aquifer (Ghebreyesus et al., 2016; Gonzalez et al., 2016; Hussein et al., 2021; Lezzaik and Milewski, 2018; Wehbe and Temimi, 2021; Wehbe et al., 2018), although multiple studies have quantified groundwater storage change, depletion rate and recharge rate using GRACE in the Arabian Peninsula (Mohamed and Abdelrahman, 2022; Fallatah, 2020; Fallatah et al., 2017; Saber et al., 2017; Seraphin et al., 2022; Moore and Fisher, 2012; Yassin et al., 2019). Derived from GRACE, the groundwater storage anomaly has showed a good replication with in-situ groundwater in multiple regions (Brookfield et al., 2018; Hu et al., 2019; Moore and Fisher, 2012; Strassberg et al., 2007; Scanlon et al., 2012; Neves et al., 2020; Rodell et al., 2004; Richey et al., 2015). This motivated us to use GRACE for quantifying groundwater recharge of the Quaternary aquifer.

Our approach can be described with the following three steps: (1) We compare the monthly timeseries of groundwater monitoring wells over the period 2010–2016 with GRACE; (2) We estimate groundwater recharge rate for the period from 2011 to 2013 using the in-situ data and compare the results with groundwater recharge derived from GRACE; (3) We correlate between the number of farms, the number of working wells, and GRACE groundwater storage change.

The estimation of groundwater recharge is challenging due to the water balance system's complexity and the high cost of installing monitoring wells (Li et al., 2019; Lin et al., 2019). The incorporation of multiple recharge approaches in the estimation of groundwater recharge can help to minimize the uncertainties caused by various validity assumptions made in the recharge estimation method (Walker et al., 2019). The study employs two approaches to estimate groundwater recharge using multiple recharge components, including rainfall percolation, irrigation return flow and fluxes. These two approaches are derived from in-situ and remote sensing data, respectively. Although it is generally recommended to use the GRACE products for regional scales (>100,000 km^2), some recent studies have showed satisfactory results, in which GRACE was applied with a smaller scale or partial grid (Hachborn et al., 2017; Liesch and Ohmer, 2016; Neves et al., 2020; Ramjeawon et al., 2022). Therefore, the specific objectives of this study are as follows:

- To examine the agreement of groundwater storage change obtained from GRACE and in situ monitoring wells;
- To assess the capability of GRACE on the detection of groundwater storage changes for small scale arid areas;
- To validate the capability of GRACE in estimating groundwater recharge by comparing with the in-situ recharge estimation method;
- To investigate potential causes of sudden changes in GRACE-based groundwater storage anomalies and see whether or not they are related to the former water/agriculture policy changes.

2. Study area

The study area is in the eastern part of the Abu Dhabi Emirate, UAE, which has an area of 11,487 km^2 as shown in Fig. 1. In this area, there are 377 groundwater monitoring wells with complete lithologic logs and drilling information, including aquifer geometry and hydrogeological properties, which are available for further analyses. Meanwhile, the region is well covered by the GRACE data product. As indicated in Fig. 2, six GRACE grids are selected to cover the study area. These grids are resampled to 0.5° × 0.5° grid resolution but have a native resolution of 3° × 3°. The six grids covering the study area are downscaled from the same 3° grid resolution. For simplicity, the magnitude of GRACE cells 4 and 5 are summed together based on their areal proportions and is presented as cell 4 in the estimation. For GRACE cells 1, 3, 4 and 6, their groundwater activities including abstraction and development are mainly in the UAE side, although they are transboundary (Izady et al., 2017). Therefore, cropping these grids within UAE would not affect the recharge estimation.

Based on the Koppen climate classification system, the UAE has a tropical and subtropical desert climate with low rainfall, high temperature, and high evaporation rate (Komuscu, 2017). The eastern region of Abu Dhabi Emirate has a mean annual rainfall that varies between 35 mm and 137 mm (Fig. 3c) depending on the location and topography, and the average annual potential evaporation rate ranges from 2000 mm to 3000 mm (Alsharhan et al., 2001; NCMS, 2021). This spatial variability in rainfall can mainly be ascribed to the topographic effect where mountainous area forces the airflow to uplift and trap moisture (Niranjan Kumar and Ouarda, 2014). Thus, the station records near mountainous areas show higher rainfall than those in the desert area.

To define the catchment boundary and identify the recharge zone, discharge zone, and water divide in the study area (Condon and Maxwell, 2015), the digital elevation model was downloaded from the Shuttle Radar Topography Mission (SRTM) website (available at https://srtm.csi.cgiar.org) (Farr et al., 2007). The Oman Mountains, which are located to the east of the study area, act as a water divide with an elevation range from 1000 m to 3000 m above mean sea level (AMSL). Within the study area, the topographic elevation ranges from <50 m to 400 m AMSL, except for Jabel Hafeet, which is 1000 AMSL (Fig. 3a).

Groundwater accumulation and movement is controlled by the physiographic setting in the study area. The Al Ain area lies near the western base of Oman Mountains about 110 km southeast of the Arabian Gulf coast. Based on the hydraulic head map recorded in 2010 (Fig. 3b), the general groundwater flow direction is from east to west. The cone of depression appears near farm areas due to the intensive abstraction (Fig. 3b).

Details related to the aquifers can be found in IWACO (1986), NDC and USGS (1996). The potential geological aquifers are alluvial deposits, Holocene sabkha, Holocene sand and gravel, aeolian sand dunes, desert plain deposits, and limestones (Fig. 3b). The unsaturated zone consists of fine sands, sandstone, and gravel (ADSWIS, 2020). The Quaternary aquifer underlain by Fars formation (Miocene age) contains deposits of materials with low permeability such as siltstones, mudstones and evaporites (Imes and Wood, 2007). The saturated thickness is 100 m on the east along the border with Oman and thins to 25 m thickness towards the west. Field measurements indicate that the depth to groundwater ranges from 20 m to >100 m (below ground level) (ADSWIS, 2020).
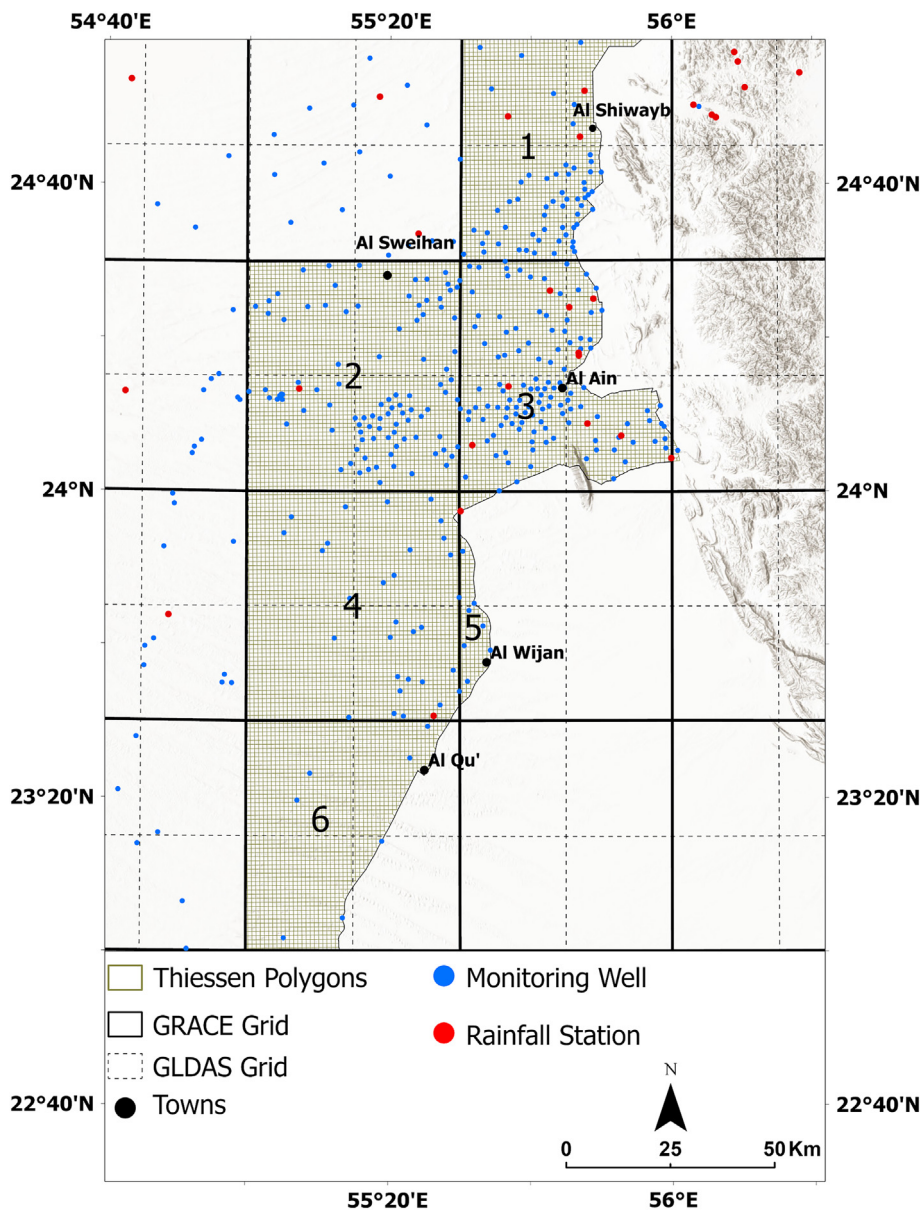
Fig. 2. The study area with the six GRACE grid cells.

3. Datasets

3.1. In-situ data

The in-situ data include the drilling information of 377 wells, subsurface hydrogeological cross-sections, aquifer test parameters, saturated thickness, rainfall data and historical water table of the study area. The collected data, from different water authorities (e.g. Environmental Agency of Abu Dhabi and National Water and Energy Centre) as well as published and nonpublished reports (Alsharhan and Rizk, 2020b; NDC and USGS, 1996; IWACO, 1986), were reviewed, validated, and stored in a GIS database as listed in Table 1. Rainfall data from 30 gauge stations located across the study area were collected from the National Centre of Meteorology and Seismology (NCMS), UAE.

3.2. GRACE data

The GRACE mission has twin satellites orbiting behind each other at an approximate distance of 200 km (Rodell and Famiglietti, 2001; Tapley

et al., 2004). This distance between them can change due to gravitational variations, but the changes are so small that a precise microwave ranging system is required to detect them. The GRACE data can be used to create average gravity field maps on a monthly basis. The gravity field signal varies whenever there is a mass change due to a change in TWS (Rodell and Famiglietti, 2001). The first GRACE mission was ended in October 2017 due to a battery issue. The GRACE Follow-On (GRACE-FO) mission was launched in April 2018 to continue the same function of GRACE.

Several GRACE products are available from different processing centers: University of Texas Center for Space Research (CSR), German Research Center for Geosciences (GFZ), the Center National D'etudes Spatiales / Groupe de Recherches de Géodésie Spatiale (CNES/ GRGS) and Jet Propulsion Laboratory (JPL) (Chambers, 2006; Bonsor et al., 2018; Tapley et al., 2004). GRACE data are available in two forms: spherical harmonics (SH) data and mass concentration solutions "MASCON" (Scanlon et al., 2016). In this study, the following four solutions have been used: (1) GRCTellus Land RL06 release of GRACE data from CSR, JPL and GFZ (available at https://grace.jpl.nasa.gov/data/get-data/monthly-mass-grids-land/) (Beaudoing and Rodell, 2020a; Landerer and Swenson, 2012); and (2) the
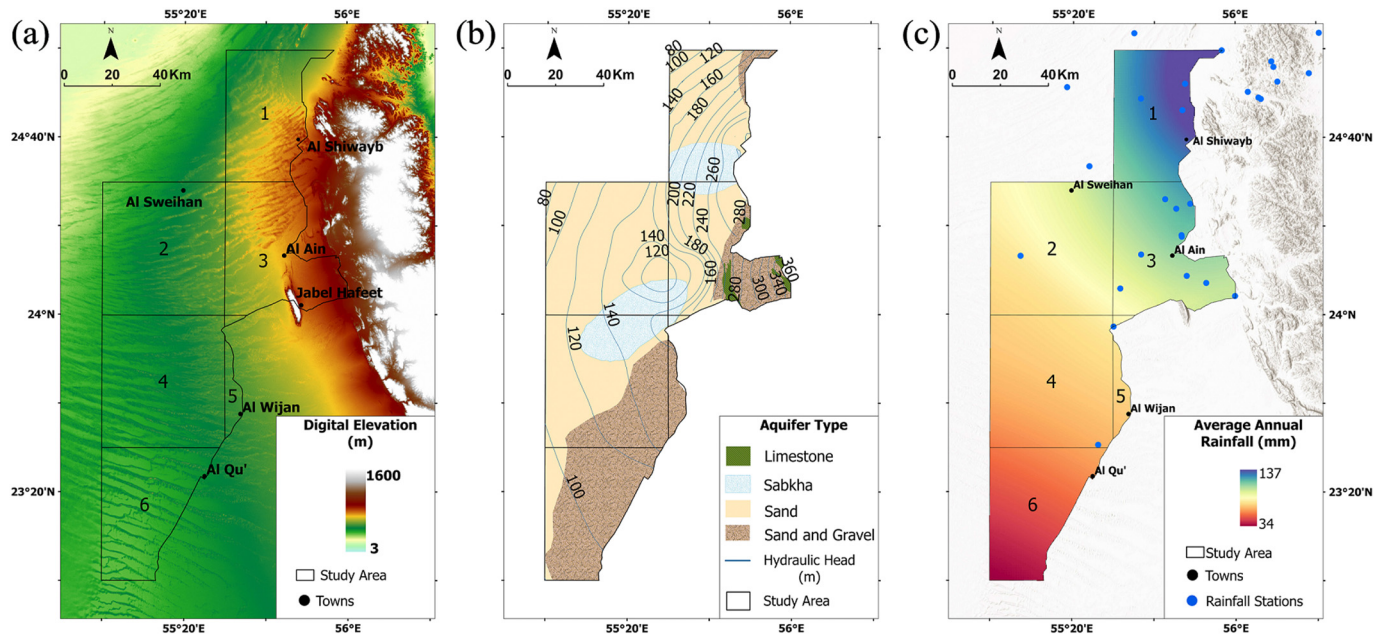
Fig. 3. Hydrological overview of the study area (a) Digital elevation model with a resolution of 30 m obtained from SRTM; this map shows mountains in the eastern region of the study area (b) Aquifer type with hydraulic head (2010) for the unconfined aquifer (c) Average annual rainfall (mm) shows the spatial variation of rainfall.

MASCON solution from JPL Release 06 Version 02 (available at http://grace.jpl.nasa.gov) (Watkins et al., 2015; Wiese et al., 2018).

The gravity solutions obtained from the three GRACE processing centers are represented by a normalized spherical harmonic coefficient up to degree and order 60. The changes in gravity field are caused due to mass movement of the solid and fluid components of the Earth system. Multiple steps are required to convert the gravity potential to Earth surface mass changes. The degree-1 coefficients represent the geocenter motion and were computed following the methods from Sun et al. (2016) and Swenson et al. (2006). The glacial isostatic adjustment (GIA) was corrected using the ICE6G-D model estimates (Peltier et al., 2018) to remove the signal from the interior Earth mass and translate the mass change from GRACE as changes in the hydrosphere (AG et al., 2013). The Atmosphere and Ocean De-aliasing Level 1-B (AOD1B) was used for the atmospheric and oceanic mass variations correction (Flechtner et al., 2015). The GRACE RL06 has better accuracy and less noise than the previous version (Release RL05) due to the improvements in the geophysical models, the data processing technique and the replacement of the Degree-2 zonal terms ΔC_{20} with a satellite laser ranging (SLR) (Cheng and Ries, 2019; Bettadpur, 2018).

The RL06 solutions obtained from CSR, GFZ and JPL are in a grid form with a spatial resolution of $1° \times 1°$. These products are based on the SH solution. To filter and truncate SH coefficients, an adjustment is needed through leakage and bias correction (Landerer and Swenson, 2012; Swenson et al., 2006). However, the adjustment might lead to some leakages and create uncertainties in the SH data. Leakage also occurs near coastal areas where signal at the land leaks into the ocean (Watkins et al.,

2015). Thus, areas near the ocean could sever with leakage which mislead reading the data. Even though applying the degree 60, destriping and 300 km Gaussian filters will remove correlated errors in the gravity solutions, this will also result in removal of energy and real geophysical signal (Cooley and Landerer, 2019; Swenson and Wahr, 2006). Therefore, the provided scaling factor is multiplied for each $1°$ grid to correct the leakage bias (also called attenuation effect) and restore the lost signal (Landerer and Swenson, 2012; Swenson and Wahr, 2006). The scale factors are derived from the modelled TWS from GLDAS Noah model (Rodell et al., 2004). In other words, leakage error was computed based on the root mean square difference (RMSD) between the GLDAS Noah terrestrial water storage estimate and the unfiltered terrestrial water storage signal obtained from GRACE. The scale factor was derived by least-square fitting between the TWS derived from GLDAS NOAH and the unfiltered GRACE (Landerer and Swenson, 2012).

The JPL MASCON (RL06) solution is defined as an equal-area $3°$ spherical cap mass concentration elements with no further postprocessing are required to remove the correlated error (Watkins et al., 2015; Wiese et al., 2016). The Coastline Resolution Improvement (CRI) filter and using the scale factors will help on reducing the leakage across the land and ocean boundaries (Wiese et al., 2016). The advantage of MASCON's data lies in the simplicity to discriminate between land and water, whereas the SH form has higher uncertainties because the signals must be restored and ocean and leakage affect correction must be applied (Cooley and Landerer, 2019). The downscaling factors from the National Centre for Atmospheric Research's Community Land Model 4.0 (NCAR CLM 4.0) (Lawrence et al., 2011) were used to restore the amplitude of terrestrial water storage and to enhance the spatial resolution from $3° \times 3°$ to $0.5° \times 0.5°$ (Gent et al.,

Table 1

Types of the collected data and sources.

Data type	Source	Spatial resolution	Native resolution	Time range	Temporal Scale
Terrestrial Water Storage	GRACE RL06 (CSR, JPL, GFZ, and JPL MASCON)	JPL MASCON $(0.5° \times 0.5°)$ CSR-GFZ-JPL $(1° \times 1°)$	JPL MASCON $(3° \times 3°)$	2003–2019	Monthly
Soil Moisture	Noah, VIC and CLM	$(1° \times 1°)$	N/A	2003–2019	Monthly
Groundwater telemetric monitoring wells	Environment Agency of Abu Dhabi	70 wells	N/A	2010–2016	Hourly
Drilling information and specific yield	National Drilling Abu Dhabi Emirate- U.S. Geological Survey	377 wells	N/A	1980–2011	N/A
Rainfall	National Centre of Meteorology and Seismology, Abu Dhabi	30 rain stations	N/A	2005–2019	Monthly

2011; Landerer and Swenson, 2012). Even though MASCON solutions were resampled to 0.5° × 0.5° grids, the native resolution of MASCONs are 3° × 3°. The major difference between spherical harmonic (SH) solutions and MASCON solutions are the adopted postprocessing technique. The SH solutions remove the noise and restore the signals by applying the destriping and smoothing filters whereas the MASCON solutions apply constraints derived from geophysical models (Scanlon et al., 2016).

The missing data due to battery issues were linearly interpolated (Cooley and Landerer, 2019). The interpolated missing data records from October 2017 to April 2018 were not accounted in the calculation of recharge to reduce uncertainty.

3.3. GLDAS hydrological model

The global land data assimilation system (GLDAS) is a land surface model that incorporates in-situ data and satellite data to simulate components of TWS changes (Rodell et al., 2004). There are four land surface models from GLDAS with different spatial resolutions (e.g., Community Land Model (CLM), Noah, MOSAIC, and Variable Infiltration Capacity (VIC)). For this research, the following monthly soil moisture storage data are used: (1) CLM (version 2.1) (Li et al., 2020), (2) Noah (version 2.1) (Beaudoing and Rodell, 2020a), and (3) VIC (version 2.1) (Beaudoing and Rodell, 2020b; Rodell et al., 2004) with spatial resolution of 1° × 1° (available at https://ldas.gsfc.nasa.gov/gldas/) are used for the groundwater calculations. The claimed vertical penetrated depth of modelled soil moisture in CLM, Noah and VIC are 3.4 m, 2 m, and 1.9 m, respectively (Bi et al., 2016) with multiple vertical profiles (Rodell et al., 2004). The three soil moisture products were averaged to reduce the uncertainties. The surface water is negligible to account for in the calculation as it is seasonal and appears during rainfall events for a short period (Sherif et al., 2021).

4. Methods

4.1. Groundwater storage changes derived from GRACE

The isolation of soil moisture (SM) from liquid water equivalent thickness (TWS) derived from GRACE helps with the calculation of groundwater storage anomaly (GWSA) (Eq.1). In the data products obtained from the four GRACE products (Fig. 4a), an averaged baseline from 2004 to 2009 is applied to the anomalies (Cooley and Landerer, 2019). Similarly, an average baseline is computed and applied for the soil moisture anomaly (Fig. 4b). Soil moisture data obtained from CLM, Noah and VIC are averaged to consider the different depth of soil profiles. Following Eq.1, the groundwater storage anomaly is calculated for the four GRACE solutions as shown in (Fig. 4c)

$$\Delta GWSA\ (L) = \Delta TWS(L) - \Delta SM(L) \tag{1}$$

In previous research, seasonal removal using a temporal filter, such as a 12-month moving average, Butterworth low-pass-filter, and Hodrick Prescott (HP) filter were applied for GRACE and exhibited a better agreement with in-situ groundwater data than the original GRACE products (Scanlon et al., 2012; Bhanja et al., 2016; Andrew et al., 2017). The use of temporal filter removes high frequency noise and seasonal fluctuation, which reduces errors in the calculation (Scanlon et al., 2012). To de-seasonalize the groundwater timeseries, the 12-month moving average was applied.

4.2. Comparisons between in situ and GRACE derived groundwater storage

Telemetry groundwater level data are obtained from the Environment Agency of Abu Dhabi to estimate the groundwater storage (GWS) changes for the comparison with groundwater storage change derived from GRACE. The retrieved groundwater monitoring wells have well screens penetrated in the surficial unconfined aquifer (Quaternary aquifer). To estimate the amount of water change within the aquifer, the specific yield is taken into account in the calculation. The specific yield represents the volume of water that a rock can retain in an unconfined aquifer. The specific yield data was provided for the chosen wells in the study area. The specific yield values varied from 0.01 to 0.3 depending on the soil type.

For the analysis, it is required to have a temporally continuous data; therefore, among the 70 telemetric monitoring wells, 40 wells were satisfying over the periods 2010 to 2016. The chosen wells have an hourly record. To match with GRACE temporal resolution, the data was aggregated from hourly to monthly. It has been observed that telemetric wells have gaps in the data due to the signal loss and battery issues. To reduce the uncertainty, the gap in the data was not interpolated nor taken into the calculation. The
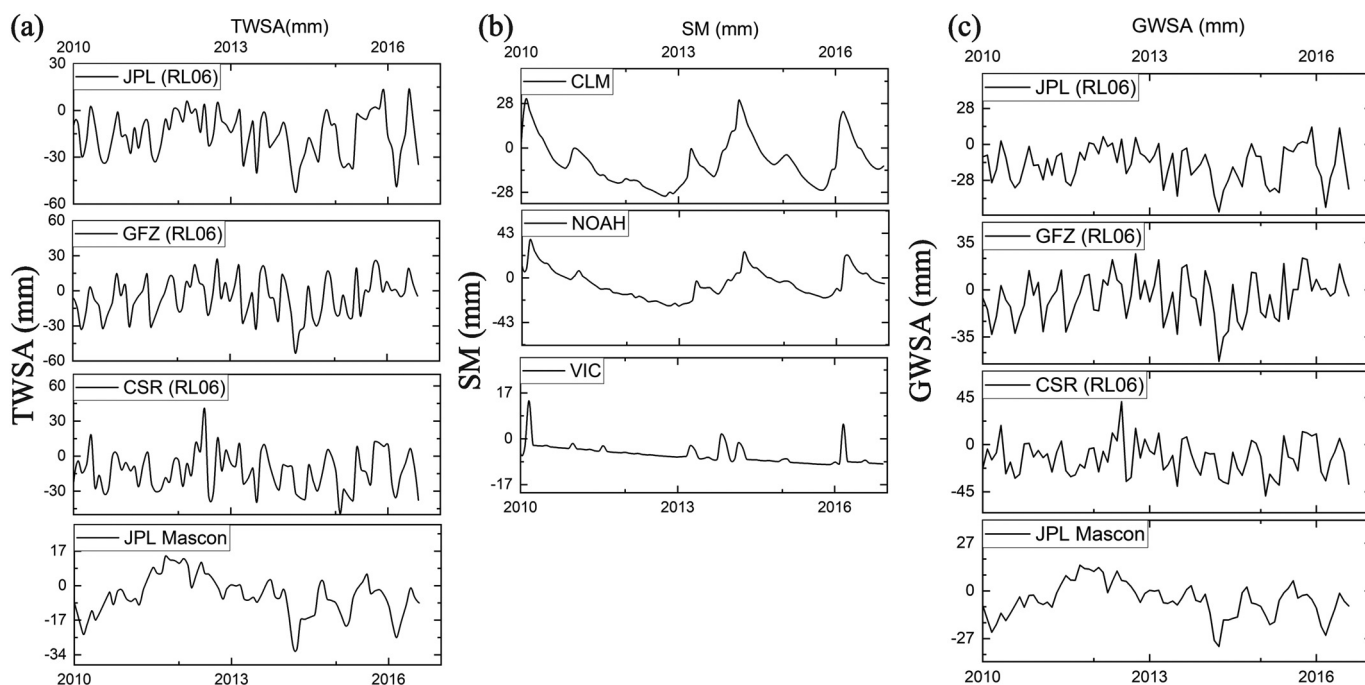

Fig. 4. (a) Terrestrial water storage anomalies from the four GRACE products (b) The soil moisture from three land surface models (CLM, Noah, and VIC) with different profile depths (c) The GWSA calculated for each GRACE product for the comparison with the in-situ groundwater storage change.

hydraulic heads for these wells varied spatially which indicate the heterogeneity of the aquifer. To compare groundwater storage change, the in situ groundwater level data was converted to groundwater storage change following Eq.2 (Todd and Mays, 2005; Bhanja et al., 2017; Bhanja et al., 2018; Hachborn et al., 2017; Swenson et al., 2006; Sun et al., 2010).

$$\Delta Groundwater\ Level = \Delta h \times S_y \qquad (2)$$

where Δh represents the hydraulic head change at different time and S_y is the specific yield of the unconfined aquifer. A comparison of the in situ GWS data with the detrended and seasonal trend of GWS-GRACE data is conducted to investigate the optimum GRACE product among the four GRACE processing centers. The Pearson's correlation and RMSE are used to validate the GRACE products that can reflect the in situ GWS changes. The autocorrelation is applied to detect if there is a lag between the two datasets. The annual seasonal trend was additionally assessed to detect the seasonality of the data over the chosen period (2010–2016). The GRACE product, which has the best match with the in-situ monitoring wells, is used for computing the groundwater recharge rate that could achieve the second objective of this study.

4.3. Multi recharge components estimation

Groundwater recharge (GWR) is known as water from rainfall or from surface water that percolates through the unsaturated zone and reaches the water table (Meinzer, 1923). In this paper, the GWR is defined to account for multiple recharge components, including rainfall, irrigation return flow, and groundwater flux. Methods proposed here will help to estimate the GWR in addition to its validation derived from the GRACE and GLDAS data. The period from 2011 to 2013 is selected for GWR due to the data availability during this period. The rainfall recharge is calculated using an empirical method, which is discussed in detail in Section 4.4. The Eq.3 below relates the multiple recharge components that were considered in the in-situ GWR:

$$GWR = Recharge\ from\ rain\ percolation + \Delta Fluxes + Irrigation\ Return\ Flow \qquad (3)$$

The GWR values derived from GRACE and the 12-month moving average applied to GRACE data were calculated by adding all the increased magnitudes within the selected years. The increase in the GRACE GWSA indicates the contribution of water fluxes to the aquifer. The accuracy of seasonal and de-seasonalized trends were investigated. The Eq.4 was used to calculate annual GRACE GWR volume, and the result was compared with the in-situ GWR (rainfall, internal flux, and irrigation return flow) result.

$$GRACE\ GWR\ (L^3) = Groundwater\ Increase\ (L) \times Area(L^2) \qquad (4)$$

4.4. Potential rainfall recharge from in situ data

The integration of multiple thematic layers to estimate groundwater potential recharge zones using GIS has been applied effectively in many regions (Kaliraj et al., 2013; Panda et al., 2021; Selvam et al., 2014). An empirical method using geospatial techniques has been used to examine the relationship between rainfall and recharge with the integration of several thematic layers in the UAE (Sherif et al., 2018). The results obtained using the empirical equation for a 1 km^2 cell were compared with and validated against the Water Table Fluctuation Method (WTF) recharge results. The WTF method is based on the rises in groundwater level after a rainfall event (Meinzer, 1923). An empirical method similar to that used by Sherif et al. (2018) was used for the study area herein to estimate the recharge from rainfall (Eq.5).

Geopotential maps were created for the following parameters: land use, soil types, drainage intersection, geology, and ground surface slope. The maximum recharge condition was recorded in a reservoir with a recharge percentage of 28 % whereas the maximum recharge percentage in the

rest of the study area was reported at 20 % (MOEW and IAEA, 2005). Thus, the 8 % difference was attributed as an augmentation factor distributed to the four different parameters (Eq.6).

The study area was divided into 11,481 grid cells ranging from 1 km^2 to 1.64 km^2, by using the Kriging method (Delhomme, 1978) to interpolate the data spatially. Before applying the Kriging interpolation to the data, the best fit variogram was developed and also cross validated.

$$Ri = \left(\left(\frac{I_i}{I_{max}} RP_{max} \right) + C_{f(i)} \right) 0.00001 P_i A_i \qquad (5)$$

$$C_{f(i)} = DI_{(i)} + GS_{(i)} + MFL_{(i)} + LU_{(i)} \qquad (6)$$

R_i: potential recharge volume for each cell (m^3)A: Cell area (1km^2)I$_i$: Infiltration rate-millimeter /hour (mm/h)I$_{max}$: Maximum infiltration rate (mm/h)PR$_{max}$: Maximum percentage recharge 20 % alluvial gravels and 0 % for infrastructureP$_i$: Average annual rainfall rate at cell I (mm)C$_{f(i)}$: Augmentation coefficient percentage of the cell [0 %–8 %]DI(i): Drainage intersection and geological structureGS(i): Ground surface slopeMFL(i): Major fault line and fractureLU(i): Land use.

4.5. Groundwater fluxes from Oman

The recharge from the Oman hydrologic basins into the study area was categorized into four types, namely Piedmont, Wadi, Gap, and Mountain front recharge. Wadi recharge occurs below the mountain gaps, whereas the other types of recharges occur above the gap. Details of these recharge values can be found in (Osterkamp et al., 1995). By using runoff simulation and water balance model techniques, Osterkamp et al. (1995) estimated a total recharge of 55 Mm^3 per year from 17 hydrologic basins in Oman to UAE. The recharge estimates obtained by Osterkamp et al. (1995) were considered as the base scenario in the predevelopment groundwater flow model relative to the other scenarios in the groundwater flow modeling study conducted by Eggleston et al. (2018). In Oman, along the border near Al Ain city, by using numerical modeling techniques, Izady et al. (2017) estimated the average annual GWR volume as 32.79 Mm^3 outflowing from Oman towards Al Ain city from six hydrologic basins. Groundwater as an internal flux moves towards the UAE through the Wadi (valley) as a transmission loss below mountain gaps. Therefore, the Wadi paths were traced to identify the contribution of internal flux to each GRACE cell (Fig. 5).

4.6. Groundwater fluxes in the UAE

For each GRACE grid cell, the Darcian approach was used to estimate the outflow and inflow (Hubbert, 1957). To estimate groundwater outflows towards the Arabian gulf, the analytical solution obtained from the Darcy's approach was applied in northern Emirates (IWACO, 1986). The results from (IWACO, 1986) by using Darcy's method (Eq.7) are similar to the outflow volumes calculated using the infrared thermal imagery method (Lavalin INC, 1980). Therefore, Darcy's method is applicable for estimating (1-D) regional longitudinal scale.

$$Q = KA\ \frac{\partial h}{\partial l} \qquad (7)$$

Q = Groundwater Flow (L^3/ T)K = Hydraulic Conductivity (L/T)A = Area of the flow (L^2)∂h = Hydraulic head change (L)∂l = The distance between the two measured wells (L).

The aquifer parameters used in the 1-D calculation following Darcy's equation such as aquifer saturated thickness and hydraulic conductivities were averaged for the generated 1 km^2 grid cell in the GIS database (Fig. 6). The Quaternary aquifer characterized as a heterogenous aquifer where the hydraulic conductivity varies spatially (Fig. 6a). The hydraulic conductivity was estimated for the transmissivity and saturated thickness from the pumping test performed in the study area (NDC and USGS, 1996). To overcome the problem of heterogeneity, the weighted average
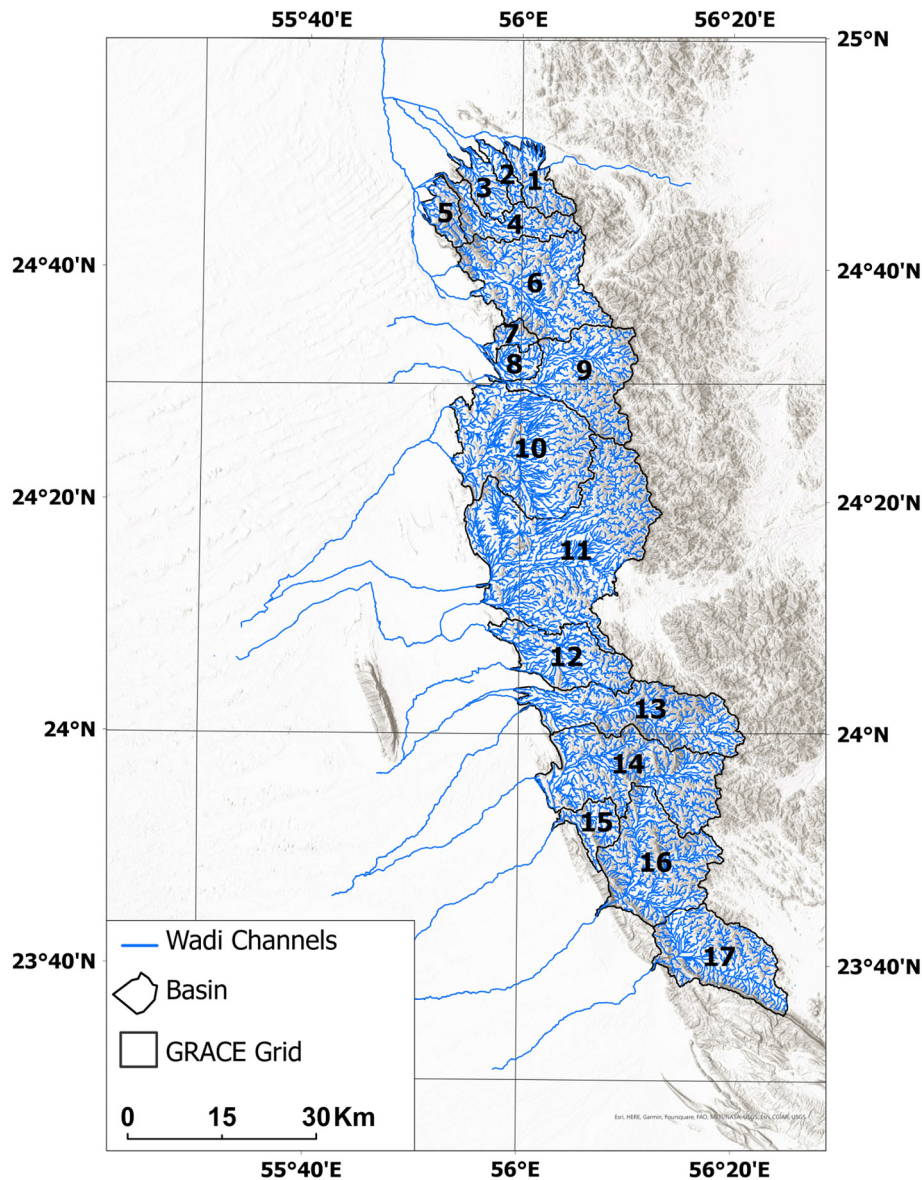
Fig. 5. The basins and wadis channels in Oman Mountains where the major wadis are clearly shown.

of hydraulic conductivity was calculated for each GRACE cell along the flow direction (Table S1). All data were gridded and fit to the variogram model after testing for the 11,481 grid cells. In this research, based on the hydraulic head values, we assumed that groundwater regionally travels in one dimension from the east to the west towards the Arabian gulf. The estimated fluxes for each cell were estimated using Eq.7.

4.7. Irrigation return flow

The agricultural area is categorized into flood irrigated and drip irrigated systems. The irrigation return flow is defined as "the excess of irrigation water that is not evapotranspirated or evacuated by direct surface drainage, and which finally returns to an aquifer" (Dewandel et al., 2008). The irrigation return flow was calculated empirically following the method outlined in PIK (2007) and the ratio is 14.5 % (Sathish et al., 2018). In arid region, by using numerical, tracers and experimental methods, the irrigation return flow for the flood irrigated system was estimated around 13 % (Naghedifar et al., 2018), 15 % (Jafari et al., 2019) and 15.2 % (Ebrahimi et al., 2016). Thus, the irrigation return flow percentage used in the calculation is 14 %.

The Department of Forestry in the UAE initiated the greening program to grow domestic trees that tolerate the arid region climate. The drip irrigation system is mainly used for the forestry where water would not infiltrate beyond the root zone due to the high evapotranspiration (Yakirevich et al., 2013). The annual irrigation rate for the forestry was estimated to be (2300) m³/ha (NDC and USGS, 1996). Therefore, the forestry area was subtracted from the total agricultural area that was not accounted for in the return flow calculation (Fig. 7). The major crop grown in the region is palm tree and the irrigation rate per hectare (1 ha = 100 palm trees) varies in the region due to the lack of knowledge of farmers to the required irrigation amount (Alomran et al., 2019). Thus, for simplicity, the irrigation rate used for the irrigation return flow calculation is averaged from multiple papers, which is 13,700 m³/ha (Al-Muaini et al., 2019; Alomran et al., 2019; Al Tenaiji et al., 2021).

4.8. Trend analysis

The seasonal Mann-Kendall trend test (M-K test), which has been widely used for hydrometeorological time series (Hamed, 2008; Shi et al., 2010), was applied for trend analysis. This method was firstly proposed by Mann
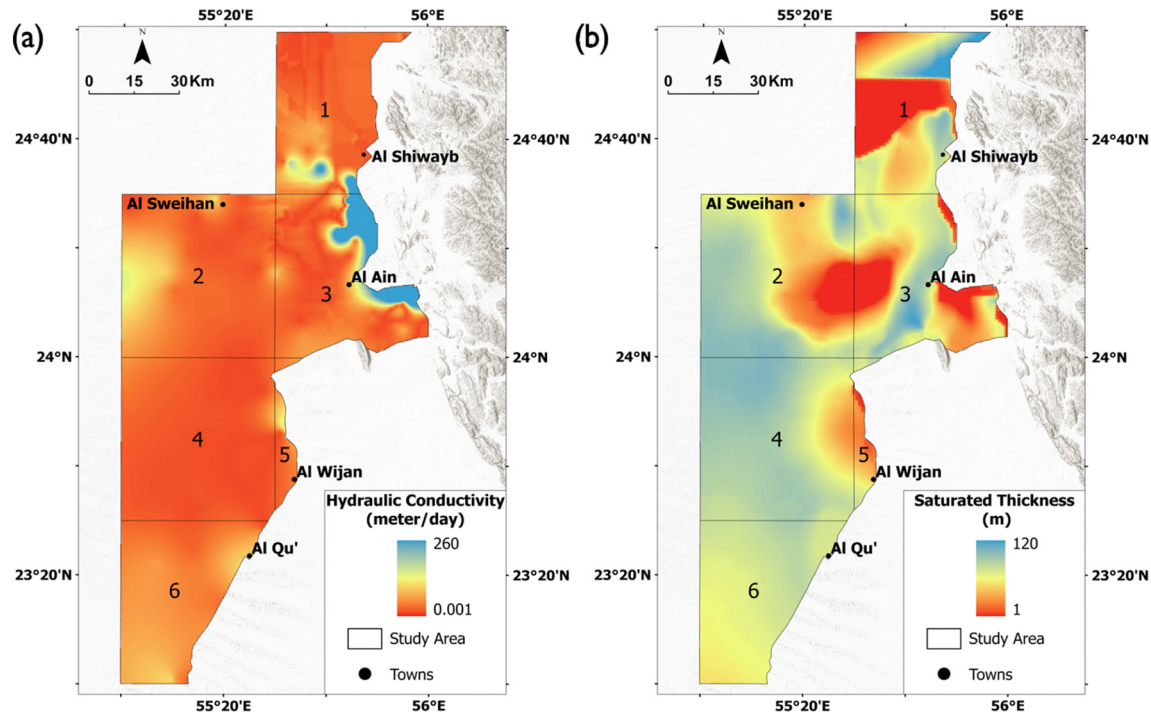
Fig. 6. Hydraulic parameters (a) Hydraulic conductivity (m/day) (b) Saturated thickness (m) used for the flow calculation following Darcy's equation.

(1945) and furthermore investigated by Kendall (1955). The M-K test and Sen (1968) Slope estimator were used to estimate the significance and trend magnitude, respectively. This nonparametric test neglects the restriction of normal distribution condition and was, therefore, applied to detect the trend and any changes in its magnitude for the GRACE GWSA. The trend detection contributed to an examination of the impacts of groundwater policies and subsidies on the GRACE GWSA. The analyses were investigated to assess the monthly trends over two periods: (a) period 1 (2003−2010); and (b) period 2 (2010–2016). The secular trend of GRACE GWSA was calculated by fitting a linear trend to the timeseries. The errors associated with the trend was estimated at a confidence interval of 95 %.

5. Results

5.1. Comparisons between GWSA derived from GRACE and in situ groundwater storage

The performance of different GRACE products is assessed by comparing them with the in situ GWS. The comparison between the in situ and GRACE products is shown in Fig. 8. The decomposed trends of GRACE and in situ monitoring wells showed better agreement than the seasonal trends. The GRACE RL06 products performed poorer in the study area compared to the JPL MASCON (Table 2). The 1-month lag showed better correlations for the 4 GRACE products. This lag is attributed to the hydrological parameters such as depth to water and the infiltration rate of the soil. Based on previous studies, a 1-month time lag has been observed in the areas with thick unsaturated zones (Wang et al., 2020; Brookfield et al., 2018). The JPL Mascon showed the highest correlation (Pearson correlation, $r = 0.5$, p value <0.05) among the four GRACE products. The RMSE for all the GRACE products were within a close range (RMSE = 11.8 mm to 18.9 mm), but JPL MASCON has the smallest RMSE. This complies with previous research, in which JPL performs better than the other GRACE products in different regions.

Averaging the monthly data was another approach to detect the seasonality. Among the 4 GRACE products, JPL mascon showed also the best seasonality performance ($r = 0.8$, $p < 0.05$). Thus, among the different GRACE solutions, JPL Mascon was chosen for the recharge rate calculation.

5.2. Potential rainfall recharge method

The computed groundwater recharge from rainfall is shown in Fig. 9c and summarized in Table S2. Based on these results, the annual rainfall and total annual recharge showed consistent spatial pattern (Fig. 9a and Fig. 9c). The highest groundwater recharge is shown in cell 1 due to the high annual rainfall received in that cell. Even though cells 4 and 6 have high infiltration rates (Fig. 9b), the groundwater recharge rates in these cells are the lowest. The applied empirical method related multiple parameters such as land use, soil types, drainage intersection, geology, ground surface slope and annual rainfall. Among these parameters, it is concluded that the amount of rainfall is a major controlling factor to recharge groundwater other than the infiltration rate. Similarly, Imes and Wood (2007) concluded that recharge is neglected near the sand dunes due to the high thickness of the sand dunes where water evaporates before reaching groundwater table. By using the water table fluctuation method, Shi et al. (2015) concluded that in New South Wales, Australia, the major factor controlling groundwater recharge following water table fluctuation method is the amount of rainfall instead of other factor such as depth to water table or groundwater level. The result from the potential recharge method (PRM) showed that the amount of rainfall is a major factor to determine the occurrence of groundwater recharge which corresponds with the previous studies (Imes and Wood, 2007; Shi et al., 2015). The results obtained using the PRM (Table S2) are incorporated into the in-situ recharge calculation method by using Eq.3. The uncertainties associated from the potential recharge method come from the interpolation method applied to generate the maps. The cross validation of the variogram model reduces the uncertainties associated with these parameters.

5.3. Groundwater fluxes

The groundwater fluxes were calculated using two methods. Along the border, the groundwater fluxes traveling from Oman below and above the gaps were estimated by tracing each wadi path and identifying the GRACE cell to which it contributes, as described by Osterkamp et al. (1995) (Table 3 and Table S3). In Al Ain city (cell 3), the recharge rate due to
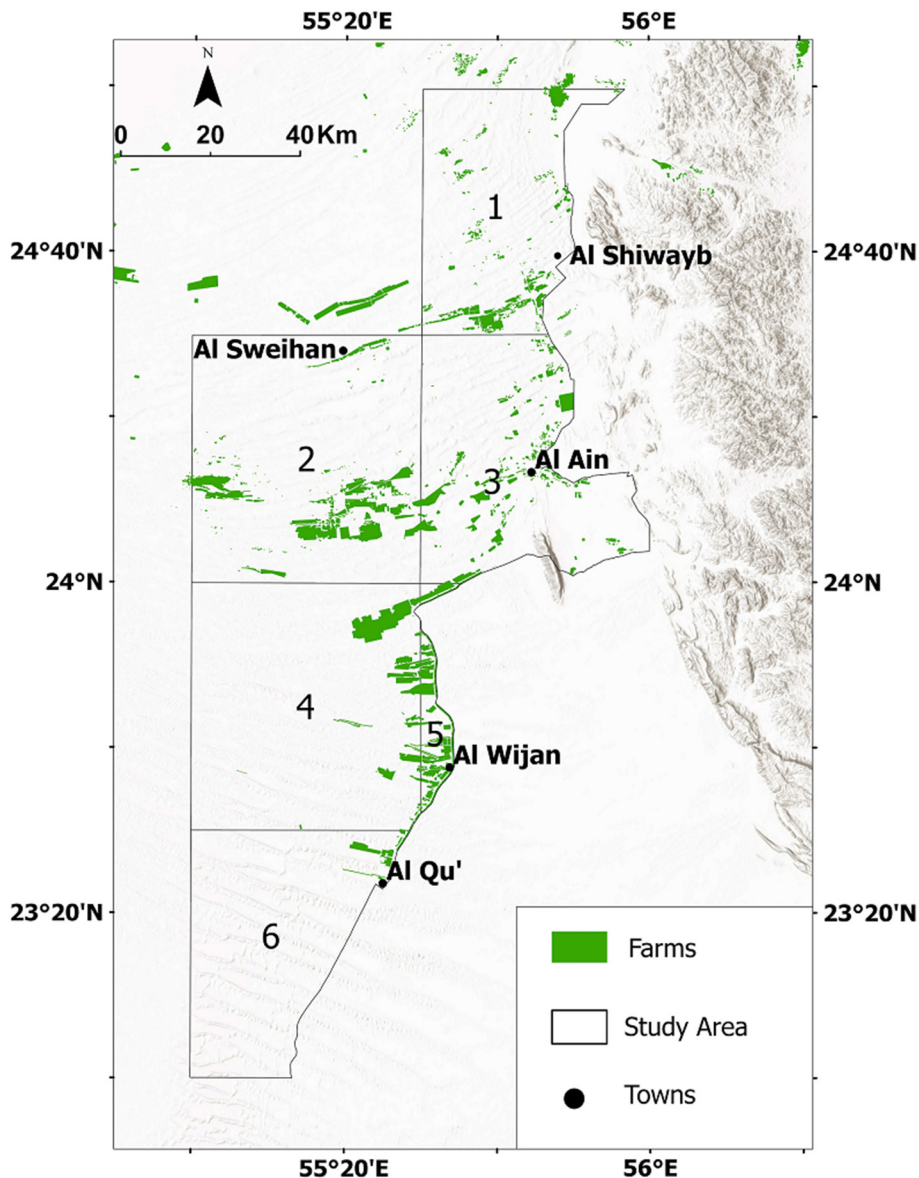
Fig. 7. Registered farms in the study area in 2011.

groundwater fluxes is the highest among the other cells due to the existence of wadi channels from the major basins from the mountains to the cell (basins 10, 11 and 12). The lowest recharge rate due to groundwater fluxes from Oman basins to the study area was recorded in cell 6 because of the large distance between the mountains and the cell and a limited number of wadi channels.

As for the other method to calculate groundwater fluxes in the study area, the analytical solution obtained using the 1-D Darcian solution was applied. Hydraulic conductivity and saturated thickness maps exhibited a spatial variability because of the heterogenous geology of the aquifer and the intensive groundwater withdrawals near agricultural areas (Fig. 6). The groundwater fluxes rates traveling out of the cells were the highest in cell 3 owing to the high hydraulic conductivity and hydraulic gradient (Table S1and Table S4). Cell 4 had the lowest hydraulic conductivity, and a low hydraulic gradient; therefore, it had the least fluxes traveling outward. A cone of depression (Fig. 6b) was found in cells 1, 2, 3, and 5, which is due to the intense agricultural withdrawals. Table S3 and Table S4 summarize the groundwater fluxes and these results were input in Eq.3.

5.4. Irrigation return flow

The final component in the recharge calculation following Eq.3 is the irrigation return flow. Most of the registered farms are in cells 2 and 5 (Fig. 7 and Table 4). The irrigation return flow percentage calculated using the method proposed by PIK (2007) was 14.5 %, which is consistent with the results of other studies conducted in arid regions (Naghedifar et al., 2018; Jafari et al., 2019; Ebrahimi et al., 2016). The irrigation return flow percentage used in this study is 14 %. Irrigation return flow mainly occurred in cells 2 and 4 (Table 4). In the absence of smart meters to calculate the abstraction rate for each farm, it is challenging to calculate the irrigation rate. Given that palm tree is the major crop grown in the region, one can obtain an estimate based on the irrigation rate per hectare for palm which is 13,700 m^3/ ha. The irrigation return flow listed in Table 4 was used for the recharge calculations by following Eq.3. For simplicity, in this study, one can reasonably assume a constant irrigation rate to roughly estimate the irrigation return flow. The uncertainty caused by assuming a constant irrigation rate and irrigation return flow percentage should be investigated further to account for the spatial variability. This task requires
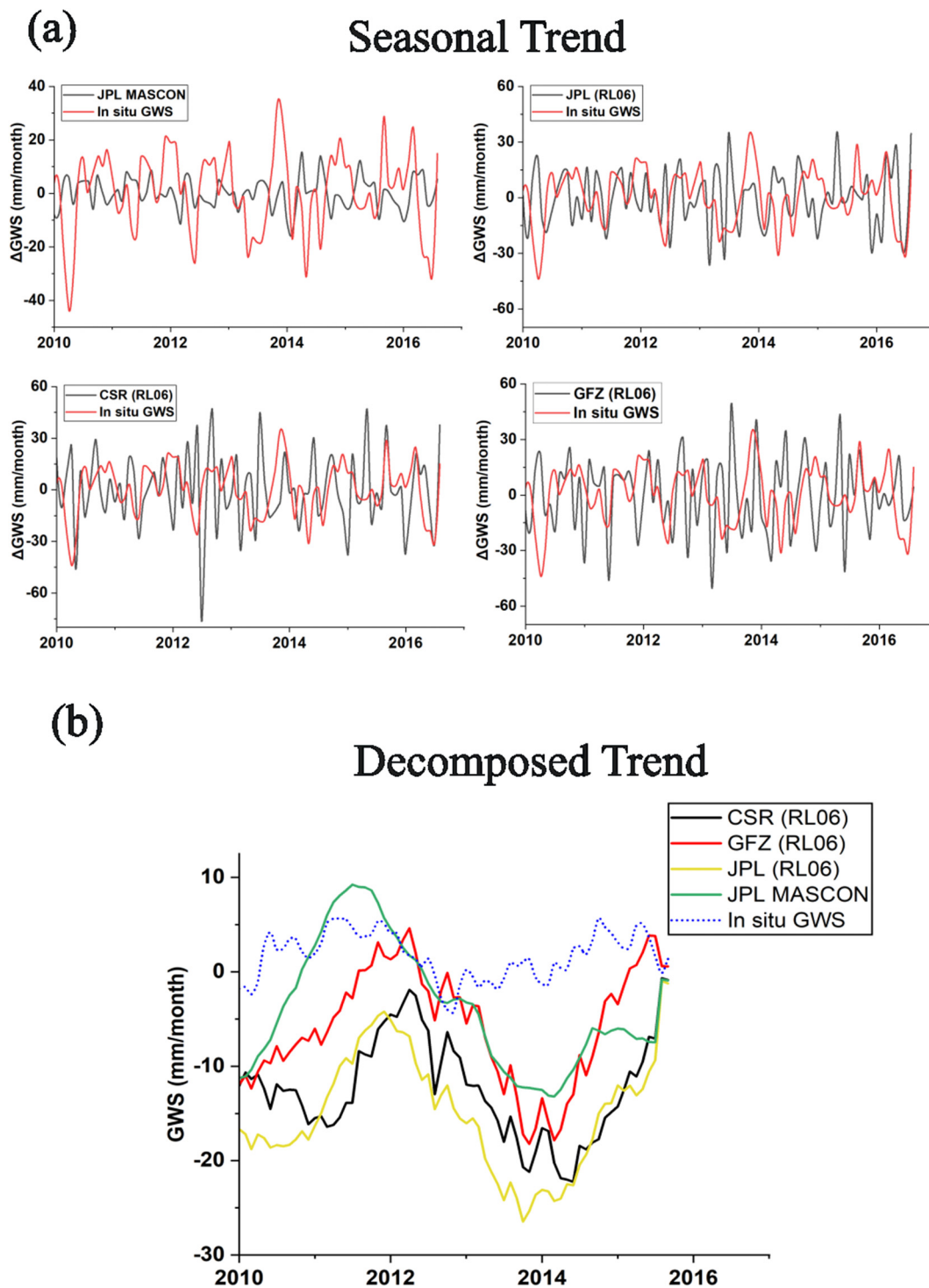
Fig. 8. (a) The timeseries calculated from different GRACE products for the study area compared with the in situ GWS; (b) The decomposed trends for the monthly data obtained from GRACE and in situ.

Table 2
Comparison of the decomposed trend (12-month moving average) obtained from the four GRACE products with the in situ GWS.

Data	R (Lag = 0)	R (Lag = 1)	RMSE
CSR RL06	<0.3	<0.3	16.7 mm
JPL RL06	0.4	0.5	18.9 mm
GFZ RL06	0.3	0.4	12.7 mm
JPL MASCON RL06	0.5	0.5	11.8 mm

an extensive analysis in terms of numerical modeling of the unsaturated zone and data collection from agencies. The uncertainties associated with calculating the irrigation return flow could vary for the study area due to the absence of smart meters in agricultural wells to estimate the pumping rate. The irrigation volume could vary yearly and the pumping patterns for individual farms could vary as well. Given that the pumping rate was obtained from multiple studies, the uncertainties associated with pumping rate falls within the confidence level of $+ - 500 \, \text{m}^3/\text{ha}$ and the irrigation return flow percentage is very minimum to consider ($\pm 0.4 \%$).
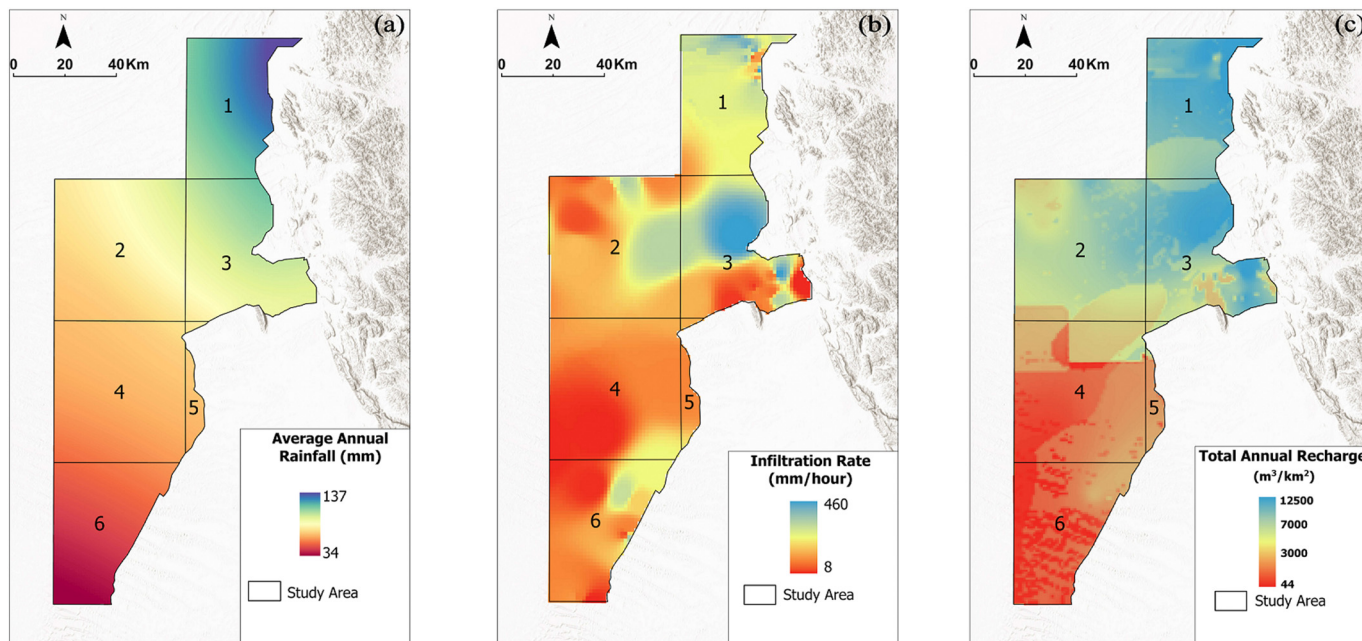
Fig. 9. Spatial distribution of (a) Annual rainfall (mm/year) (b) Infiltration rate (mm/h) (c) Annual recharge (m^3/km^2) calculated using PRM.

5.5. Recharge estimation from all in-situ recharge components

The results obtained using the in-situ recharge approach relate several recharge components and provide valuable insights into the study area (Table 5). Rainfall recharge does not contribute substantially to the recharge for cells 4 and 6, but internal flow and irrigation return flow are the major recharge sources. Cell 2 has the highest proportion of agricultural area; therefore, it is expected to have the highest recharge rate due to irrigation return flow. This understanding of the hydrogeological features and agricultural practices within the study area helped to calculate recharge values. Knowledge of the recharge values and sources for each GRACE cell is important for validating the GRACE and GLDAS data, and for sustainable water resources management.

5.6. Groundwater recharge from GRACE

The recharge estimation derived from GRACE is averaged for the years 2011, 2012 and 2013 to ensure a match with the period considered in the in-situ recharge estimation approach. The GWSA of the five downscaled cells show similar trend variations, but there exist differences in the amplitude (Fig. 10a and Fig. 10b). These small changes in amplitude are ascribed to local recharge or discharge in a cell. Even though the study area (11,487 km^2) is small scale in view of the recommended footprint of GRACE (~100,00 km^2), the groundwater recharge in the five cells exhibited spatial variability. The gap between GRACE and GRACE FO is shown clearly in Fig. 10a, but it was not used in the calculation. GRACE and GLDAS were able to capture the timing of rainfall events (Fig. 10c). Groundwater recharge was the highest in cell 1 whereas cells 4 and 6 have the least

groundwater recharge (Table 6). The groundwater recharge estimates in Table 6 were compared with the in-situ recharge results in Table 5 to examine the accuracy of GRACE.

5.7. Comparison between in-situ and GRACE groundwater recharge

The results obtained from the in-situ recharge approach were compared with the groundwater recharge values obtained from GRACE data. The seasonal trend did not show good agreement with the in-situ recharge estimation method ($R^2 = 0.43$, RMSE ranges from 47 to 79 Mm^3), whereas the de-seasonalized timeseries performed using the 12-month moving average exhibited better agreement ($R^2 = 0.91$, RMSE = 1.5 to 7.8 Mm^3) (Table 7). Additional matrixes have been used to evaluate the accuracy of GRACE product against in situ data. The following matrixes have been applied to the calculation: Nash-Sutcliffe efficiency (NSE) (Nash and Sutcliffe, 1970), Percent bias (PBIAS) and RMSE-observation standard deviation ratio (RSR). The NSE is 0.7, which is within the acceptable level of performance. The PBIAS is 4.5 % indicating an underestimation bias of the de-seasonalized GRACE product, whereas the RSR is 0.5 Mm^3. These different matrixes helped on evaluating the performance of GRACE on estimating groundwater recharge rate. These results are remarkably validating the GRACE JPL MASCON and GLDAS products. The main purpose of using these two approaches to estimate groundwater recharge is to reduce the uncertainty of each method.

GLDAS soil moisture has limitation to detect soil moisture penetrated up to 3.4 m depth. The depth to groundwater in the study area varied from 20 m to 140 m (ADSWIS, 2020). This scenario implies that a large volume of soil moisture may not be within the coverage of GLDAS (below 3.4 m

Table 3
List of GRACE cells for which the recharge value was estimated as an internal flux from the basin.

GRACE Cell No	Hydrologic Basin No
1	1-2-3-4-5-6-7-8-9
3	10-11-12
4	13-14-15
6	16-17

Table 4
Irrigation return flow based on a 14 % return flow rate.

Cell ID number	Farm area (ha)	Irrigation rate per year (Mm^3)	Return flow (Mm^3)
1	5812	79.6	11.1
2	10,741	147	20.58
3	4167	57	7.99
4	10,389	142	19.8
6	786	10.7	1.5

Note: Palm is the major crop grown and the irrigation rate is 13,700 m^3/ha.

Table 5
Summary of in-situ groundwater recharge calculation considering multiple components

Cell ID	Irrigation return flow (Mm³)	Potential recharge method (Mm³)	Internal flow (Mm³)	Outflow (Mm³)	Total In-Situ Groundwater Recharge (Mm³)
1	11.1	13.6	13.2	9.7	28.2
2	20.58	8.2	12.7	3.6	37.9
3	7.99	11.0	19.7	12.7	25.99
4	19.8	1.1	12.3	0.6	32.6
6	1.5	0.2	10.0	0.8	10.9

depth) and during the isolation of soil moisture from GRACE, this volume is considered groundwater. Thus, a time lag was detected between the groundwater storage anomaly derived from GRACE and in-situ groundwater measurements in arid regions (Wang et al., 2020). Brookfield et al. (2018) indicated that the High Plains aquifer has a weaker relationship with the TWS derived using GRACE data than the overlaying alluvial aquifer due to the deep unsaturated zone in the High Plains aquifer. Similarly, this is also revealed in cell 2, where near the cone of depression, the depth to groundwater table is around 140 m and resulted in a higher RMSE compared to the other cells (Table 7). The depth to water in cell 3 is the lowest compared to the other cells; therefore, it has lower RMSE.

This demonstrates the importance of considering the vadose zone in the calculation when dealing with deep unsaturated zones. Both GRACE and in-situ recharge calculations could have limitation due to the lack of information about the unsaturated zone.

As for groundwater storage derived from GRACE and GLDAS data, the improvements of satellites to detect soil moisture at depths exceeding the 3.4 m can provide accurate estimates of groundwater recharge in area with thick unsaturated zone. Soil moisture satellites and land surface models have been developed rapidly to finer resolution reaching 0.1° or higher, but the depth remains to about 3.4 m. In terms of in-situ data, numerical modeling and sensitivity analysis of the saturated and unsaturated zones will deliver superior estimate of the dynamics of water in the unsaturated zone.

Cell 6 has a large uncertainty (RMSE 7.8 Mm³) which may be a result of the oil activities in Oman and UAE. Within Cell 6, in Oman, there are Safah and Lekhwair oil fields (Ali et al., 2017). To extract crude oil, a large volume of water is pumped from the deep carbonated aquifer. It is estimated that to produce one barrel of oil, 2–10 barrels of water are produced (Hagström et al., 2016). The oil produced water is injected into the Oligo Miocene clastic unit underlying the surficial unconfined aquifer, which increases the potentiometric head and potentially causes an upward leakage into the overlying Quaternary aquifer. (NDC and USGS, 1996). Hence, this large uncertainty is potentially related to the oil production practices and causes a mass change in cell 6. Similarly, in Sudan, GWSA
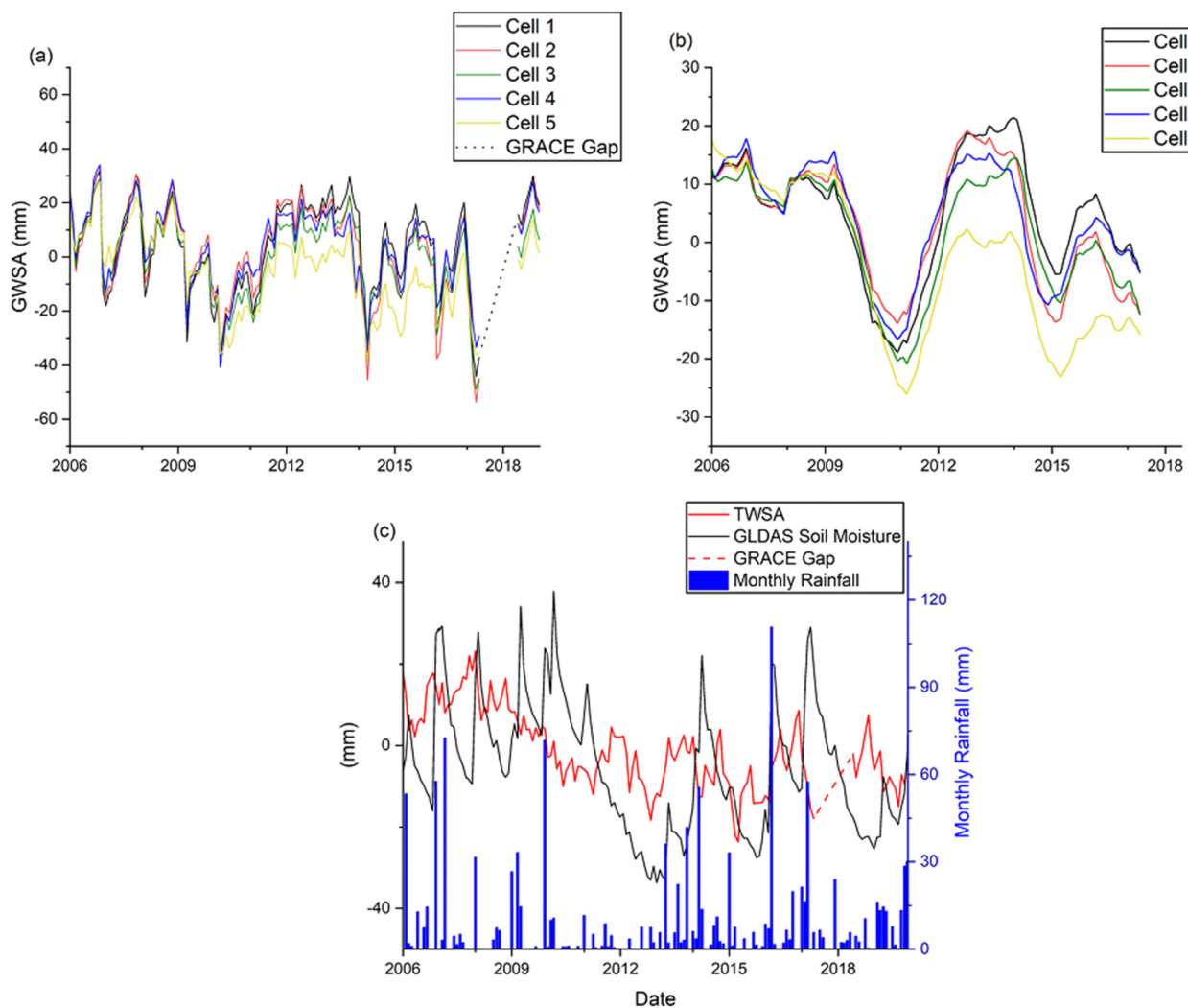
Fig. 10. a) GRACE seasonal groundwater storage anomaly (GWSA); b) 12-Month Moving Average of GRACE GWSA; c) Comparison of GRACE TWSA, GLDAS soil moisture and in-situ rainfall.

Table 6
Groundwater recharge estimation using GRACE data.

GRACE Cell ID No	Area covered (km^2)	Groundwater increase deseasonalized trend (mm)	Groundwater recharge Mm^3
1	1767	13.7	24.2
2	2826	11.3	31.9
3	1995	12.3	24.5
4–5	3031	10	30.3
6	1868	10	18.7
Total	11,487	57.3	129.7

derived from GRACE showed an agreement with the oil and water extraction data (Gido et al., 2020). This will need further investigation to understand the impact of oil field on GRACE anomalies change.

5.8. GRACE groundwater storage trend analysis

Since GRACE data is validated, one can incorporate GRACE products to evaluate the historical groundwater storage change. A comprehensive analysis of farm areal changes, GRACE GWSA, number of working wells and policies was performed to find relationship between these variables. A significant negative trend was found for the GRACE GWSA at the 5 % significance level. The estimated groundwater depletion rate from GRACE over the periods 2003–2019 is -2.43 ± 0.24 mm/year. The depletion rate was calculated for each GRACE cell to evaluate if cells covering farm areas will detect the massive depletion rate. (Table 8). Even though field data shows that cell 6 has low groundwater abstraction compared to the other cells, GRACE shows a contradictory result by having the highest decline (-2.9 ± 0.2 mm/year) over the period 2003–2019 which it could be attributed to the oil activities. The linear trend, Sen's slope and RMSE indicated the availability of another factor impacting this cell.

In the 1990s, a mass expansion in agriculture backed by huge subsidies to reduce the emirate's dependency on imports of vegetables and animals' feeds was announced by the government. Rhodes Grass was the major crop grown from 2005 to 2010, until the subsidies were ceased in 2010. In 2012, the cultivation of Rhodes grass declined by 90 %, whereas the cultivation of alfalfa declined by 75 % compared to the respective levels in 2010 (Fragaszy and McDonnell, 2016).

Based on the data obtained from the Statistics Center of Abu Dhabi (SCAD), the area covered by farms increased in the region over the period (1998–2010) from 277 km^2 to 441 km^2 (Fig. 11b) (SCAD, 2020). Similarly, within the study area, between 1998 and 2010, the number of working wells increased dramatically from 22,400 to 51,000 wells (Fig. 11a) because of the subsidies for installing groundwater wells and the guaranteed buyer for products that is the government. The estimated groundwater depletion rate derived from GRACE is -6.36 ± 0.6 mm/ year over the period from 2003 to 2011 (Fig. 11c). When the subsidies stopped and alfalfa cultivation was restricted owing to its high water consumption, in 2010, the number of working wells decreased from 51,000 to 38,000 wells over the period 2010–2015 (SCAD, 2020). This indicated a reduction in the abstraction rate. Due to subsidies cut and the implementation of a new groundwater regulation in 2010, the groundwater depletion rate derived from GRACE after 2010 to 2019 was lower (-1.28 ± 0.6 mm/ year)

Table 7
Recharge results from the in-situ and de-seasonalized GRACE methods.

Cell ID no.	In-situ groundwater recharge (Mm^3)	GRACE deseasonalized (Mm^3)	RMSE (Mm^3)	GRACE Seasonal (Mm^3)	RMSE (Mm^3)
1	28.2	24.2	4.2	75.9	47.7
2	37.9	31.9	5.9	117.6	79.7
3	25.9	24.5	1.5	80.5	54.6
4	32.6	30.3	2.2	88.5	55.9
6	10.9	18.7	7.8	76	65.1
Total	135.6	140.8	6.19	438.5	302.9

Table 8
The magnitude of the trends estimated over two periods (2003 − 2011) and (2011–2019).

Cell ID	Period 1(2003–2011)		Period 2 (2011–2019)	
	Sen's slope (mm/year)	Linear trend (mm/year)	Sen's slope (mm/year)	Linear trend (mm/year)
1	−5.61	−8 ± 0.6	−0.9	−0.8 ± 0.6
2	−5.13	−6.3 ± 0.6	−1.6	−1.5 ± 0.6
3	−6.07	−8.1 ± 0.5	−1.7	−1.4 ± 0.5
4	−5.18	−6.2 ± 0.6	−0.5	−0.4 ± 0.5
6	−6.7	−7.9 ± 0.4	−0.3	−0.2 ± 0.4

(Fig. 11c). This emphasizes the positive impact of the new regulation in the eastern region of Abu Dhabi Emirate.

Thus, by analyzing GWSA-GRACE timeseries, one can understand how GRACE was able to detect the large mass change signal, even though the area was small. GRACE signals have poor spatial resolutions, but in areas with high abstraction rates and dramatic water changes, the large mass changes allow the GRACE signals to detect changes even over smaller areas (Scanlon et al., 2012). Number of wells, annual farm areas change, government policies and GWSA-GRACE showed an agreement which is another way to validate the accuracy of GRACE products.

5.9. Uncertainty analysis

The uncertainties associated with GRACE satellites are from: (a) atmospheric correction; (b) leakage error; and (c) instrumentation error (Seo et al., 2006),whereas soil moisture data retrieved from GLDAS are associated with uncertainties due to the model parametrization, the model algorithm, meteorological forcing data, and the lack of representing human anthropogenic activities. (Bi et al., 2016). The scale factors applied to GRACE data reduced the uncertainty from leakage error.

The uncertainty analyses derived from GRACE and GLDAS were performed, and the confidence bounds of monthly TWS and SM are $\pm$ 14 mm and $\pm$ 11 mm respectively (at the 95 % confidence level) over the period 2010–2016. The linear regression between the different GRACE products showed a consistency (R^2 = 0.6) except between JPL MASCON and GFZ (R^2 = 0.2). The TWS showed similar standard deviation for the three GRACE RL06 solutions whereas the JPL MASCON has a standard deviation smaller by a magnitude of 2 (Fig. 12a). This difference in magnitude is attributed to different processing methods that the MASCON data adopted.

The range of soil moisture values obtained from CLM, Noah, and VIC is displayed as a box plot as shown in Fig. 12c. Based on the linear regression, a consistency appeared between CLM with Noah (R^2 = 0.6) and CLM with VIC (R^2 = 0.5), whereas Noah with VIC showed a weak relationship (R^2 = 0.02). VIC showed a lower standard deviation as compared to CLM and Noah by a magnitude of 2. Thus, the average value of these three soil moisture products is recommended to reduce the uncertainties.

The uncertainty of GRACE and GLDAS with the in situ GWS is computed and plotted as a shaded color in Fig. 12d. Additional uncertainty assessments associated with GRACE are implemented by considering the multiple GRACE solutions and comparing them with the in-situ data.

In situ monitoring wells increased the reliability of validating the GRACE data. The telemetric data can reduce human errors in field measurements, but missing data for certain months will increase the weight of other wells that have records. The errors associated with the chosen specific yield for each monitoring well could cause uncertainties on computing the GWS change. A change of ± 0.04 for a given specific yield of 0.08 could amplify the GWS change by 50 %. The specific yield value used in estimating GWS change was not constant. Instead, we have used a value based on the nearest pumping test applied from the drilled wells as shown in Fig. 2. The values of specific yield have a mean of 0.09 with a standard deviation of 0.05, indicating the heterogeneity of the aquifer.
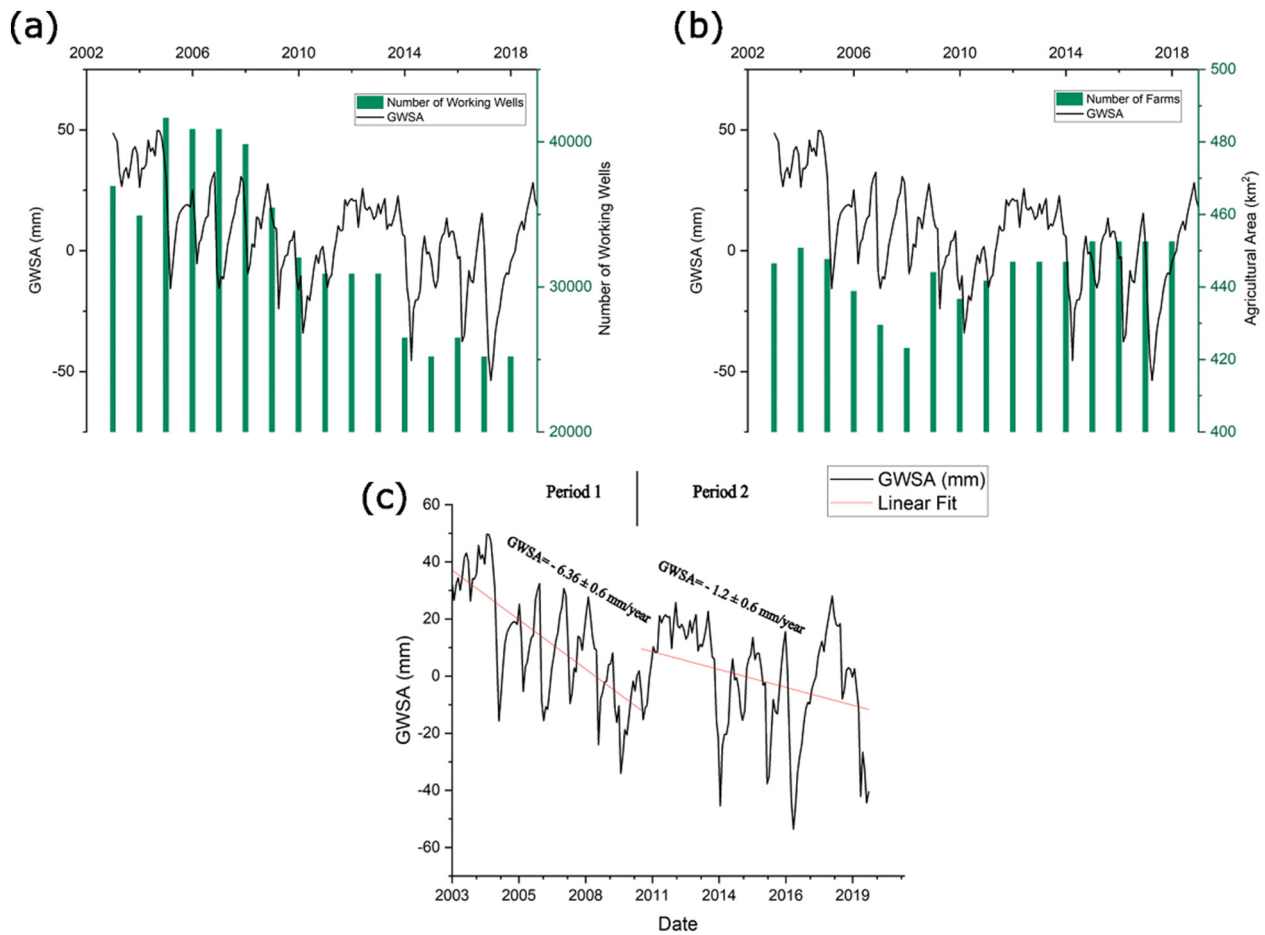
Fig. 11. Timeseries of GWSA with the (a) Registered number of wells and (b) Farm area within the region (c) GWSA trend with two linear trends before and after the subsidy cut.

To evaluate the impact of subsidy, we have used both the linear trend and the M-K test. The linear trend was represented with the uncertainty of least square fitting error. The Sen's slope was also applied to assess if a disagreement would occur when evaluating the GWS change over the two periods (2003–2010 and 2010–2019).

6. Discussion

In the UAE, some previous studies have estimated water storage or groundwater storage by using GRACE (Gonzalez et al., 2016; Ghebreyesus et al., 2016; Wehbe and Temimi, 2021; Wehbe et al., 2018; Lezzaik and Milewski, 2018), but none of them applied a detailed hydrological analysis. It is necessary to comprehensively understand the regional hydrological cycle and the aquifer characteristics within the basin. For example, Gonzalez et al. (2016) and Ghebreyesus et al. (2016) neglected groundwater flows from Oman and assumed that it is minimal to consider, but previous hydrogeological studies using numerical modeling have estimated that annually 32–55 Mm^3 of groundwater flows towards the eastern region of UAE from Oman (Izady et al., 2017; Osterkamp, 1995). Some studies compared the GRACE TWS (grid cell resolution 110 km × 110 km) with the in-situ groundwater monitoring wells data at a local scale (1000 km^2), which showed a significant negative trend (Wehbe and Temimi, 2021) and a correlation of 0.53 (Wehbe et al., 2018). In these studies, however, the separation of surface water and soil moisture from the terrestrial water storage (TWS) is neglected. The vadose zone plays an important role in the TWS variability (Rodell and Famiglietti, 2001) and should be taken into account carefully.

In our research, the groundwater inflow from Oman contributed substantially to the results obtained using multi-recharge components approach. The validation of GRACE data would help water managers to consider the use of remotely sensed data for evaluating regional groundwater resources in arid regions, even in the case of a transboundary aquifer, where data acquisition could be an obstacle. In order to gain an overall knowledge of the groundwater storage change, GRACE can be used for the areas where there is a lack of historical groundwater information. GRACE products cannot replace the in-situ monitoring wells in the regions with thick unsaturated zones owing to the limited capability of satellites to detect deep soil moisture and its coarse spatiotemporal resolution.

For smaller areas below the footprint of GRACE (100,000 km^2), the application of GRACE has been validated to estimate groundwater storage changes (Biancamaria et al., 2019; Ouma et al., 2015; Liesch and Ohmer, 2016; Rahimzadegan and Entezari, 2019; Ramjeawon et al., 2022). The direct comparison between a single GRACE grid with in situ data has been used in previous studies (Yin et al., 2020; Neves et al., 2020). In addition, the GRACE JPL MASCON data was downscaled to a 0.5° × 0.5° spatial resolution from the original 3° × 3° spatial resolution (Cooley and Landerer, 2019). Within the study area, even though the temporal pattern of GWSA derived from GRACE and GLDAS was similar for the 5 cells, it exhibited different annual amplitude, and this was interpreted as a local recharge. The partial grids along the national border with Oman exhibited a similar temporal pattern for those five grids with different annual amplitudes.

Incorporating in-situ soil moisture data in a depth exceeding 3.4 m into the calculation is another research direction. Further understanding for soil moisture deeper than 3.4 m could give a better estimation and eventually will give a better estimation to groundwater.

The results from GRACE indicated that oil production activities have a major effect on the recharge estimation. Therefore, GRACE could help on monitoring the impact of oil production on groundwater storage and
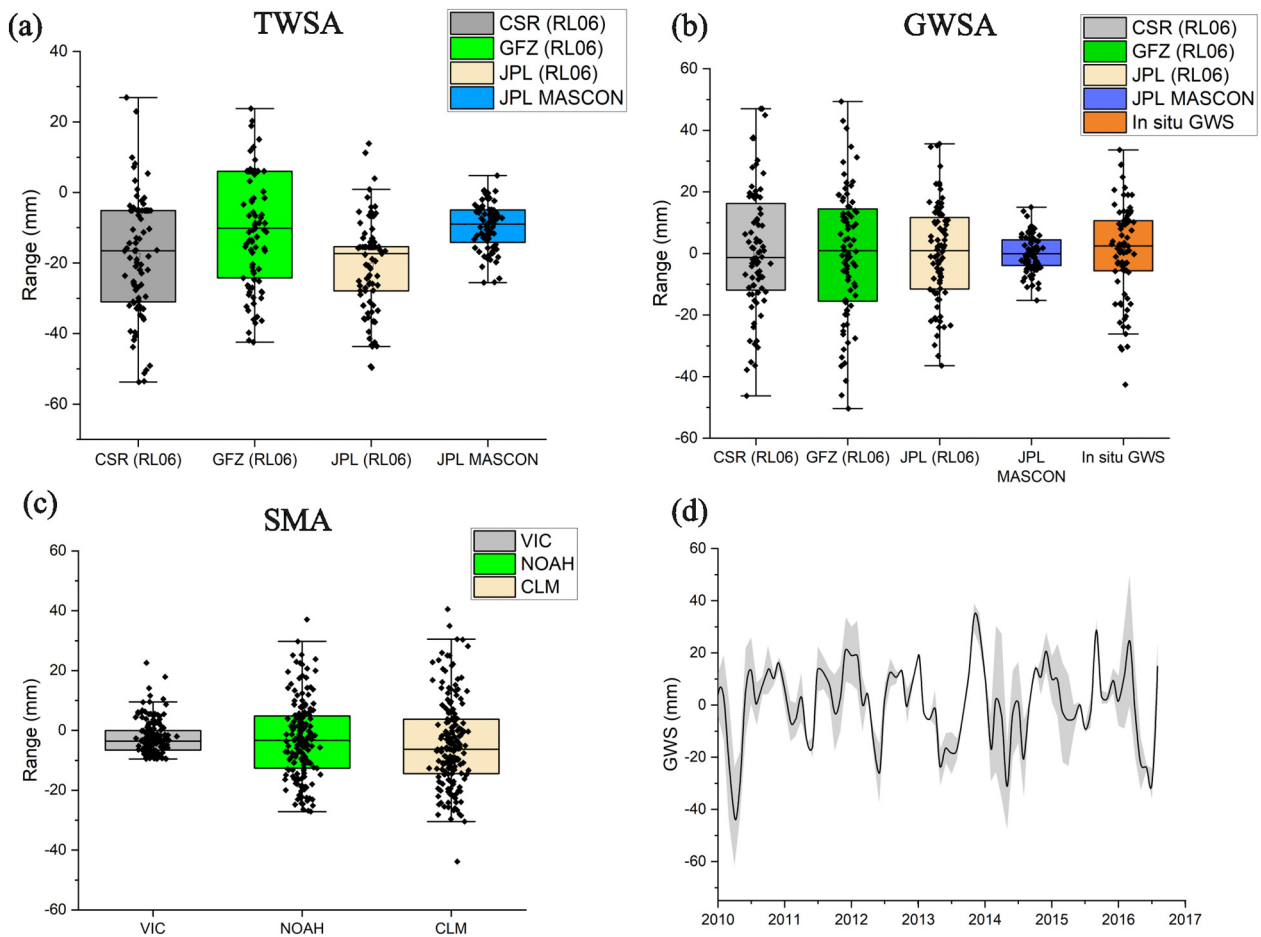
Fig. 12. GRACE and GLDAS data over the period 2010–2016 plotted as a boxplot for (a) TWSA; (b) GWSA; (c) SMA; (d) the groundwater storage change (black line) estimated from in situ and the light shaded area representing the uncertainty from GRACE and GLDAS.

recharge. The deficit between GRACE and the in-situ approach in cell 6 (7.8 Mm^3/year) could be attributed to the recharge due to the injection of oil produced water to this cell. Thus, further investigation on the oil practices and production data in cell 6 is needed. For our study, due to the multiple recharge components and its significance value, we were able to quantify these values remotely using GRACE.

7. Conclusion

Among the four GRACE products, the JPL MASCON has shown satisfactory results when compared with the in-situ monitoring wells. By using the GRACE and GLDAS products, an approach for computing groundwater recharge was developed in this study, which can help to monitor and predict groundwater resources in the UAE. The results between the in-situ recharge approach derived from multiple sources (e.g., rainfall, internal flux and irrigation return flow) and de-seasonalized timeseries using the 12-month moving average showed strong correlations (e.g., R^2 = 0.91, RMSE = 1.5 Mm^3 to 7.8 Mm^3), while the seasonal trend did not show a good agreement with that from the in-situ recharge estimation method (R^2 = 0.43 and RMSE ranging from 47 Mm^3 to 79 Mm^3). The errors between the in-situ method and remote sensing approach can be attributed to some anthropogenic practices, such as agricultural expansion and oil productions as they were clearly noted in the areas with thick unsaturated zones and/or oil production activities.

In this research, GRACE is validated quantitively and qualitatively for detecting the horizontal and vertical movements of groundwater. The massive groundwater volume depletion was captured by GRACE resulting from

the intensive agricultural practices from 2002 to 2011. By using the M-K trend test, Sen's slope and linear trends, the analysis of policies introduced by the UAE government after 2011 have shown their effectiveness to preserve groundwater resources. Therefore, the application of GRACE for recharge estimation in the arid regions can be used to support the decision-making process.

Data availability

All in situ data and post processed data from satellites will be made available at the University of Glasgow' Enlighten repository following peer review of this manuscript.

Declaration of competing interest

The authors declare that they have no known competing financial interests or personal relationships that could have appeared to influence the work reported in this paper.

Acknowledgements

Appendix A. Supplementary data

Supplementary data to this article can be found online at https://doi.org/10.1016/j.scitotenv.2023.161489.

References

Abbott, B.W., Bishop, K., Zarnetske, J.P., Minaudo, C., Chapin, F.S., Krause, S., Hannah, D.M., Conner, L., Ellison, D., Godsey, S.E., Plont, S., Marçais, J., Kolbe, T., Huebner, A., Frei, R.J., Hampton, T., GU, S., Buhman, M., Sara Sayedi, S., Ursache, O., Chapin, M., Henderson, K.D., Pinay, G., 2019. Human domination of the global water cycle absent from depictions and perceptions. Nat. Geoscience 12, 533–540.

ADSWIS, 2020. ADSWIS. In: Dhabi, E.A.O.A. (Ed.), Abu Dhabi Soil and Water Information System.

AG, Wahr, J., Zhong, S., 2013. Computations of the viscoelastic response of a 3-D compressible Earth to surface loading: an application to Glacial Isostatic Adjustment in Antarctica and Canada. Geophys. Journal International 192, 557–572.

Al Tenaiji, A.K., Braimah, N., Sgouridis, S., 2021. Impacts of farming practices on water resources sustainability for arid lands: the case of Abu Dhabi. Int. J. Water Resour. Dev. 37, 584–602.

Ali, M.Y., Fairhead, J.D., Green, C.M., Noufal, A., 2017. Basement structure of the United Arab Emirates derived from an analysis of regional gravity and aeromagnetic database. Tectonophysics 712–71, 503–522.

Al-Muaini, A., Sallam, O.M., Green, S., Kennedy, L., Kemp, P., Clothier, B., 2019. The blue and grey water footprints of date production in the saline and hyper-arid deserts of United Arab Emirates. Irrig. Sci. 37, 657–667.

Alomran, A., Eid, S., Alshammari, F., 2019. Crop water requirements of date palm based on actual applied water and penman-monteith calculations in Saudi Arabia. Applied waterScience 9.

Alsharhan, A.S., Rizk, Z.E., 2020. Climate conditions and their impact on water resources. In: Alsharhan, A.S., Rizk, Z.E. (Eds.), Water Resources and Integrated Management of the United Arab Emirates. Springer International Publishing, Cham.

Alsharhan, A.S., Rizk, Z.E., 2020b. Water Resources and Integrated Management of the United Arab Emirates. Springer International Publishing.

Alsharhan, A.S., Nairn, A.E.M., Alhajari, S.A., Rizk, Z.A., Bakhit, D.W., 2001. Hydrogeology of an Arid Region: The Arabian Gulf and Adjoining Areas. Elsevier Science.

An, L., Wang, J., Huang, J., Pokhrel, Y., Hugonnet, R., Wada, Y., Cáceres, D., Müller Schmied, H., Song, C., Berthier, E., Yu, H., Zhang, G., 2021. Divergent causes of terrestrial water storage decline between drylands and humid regions globally. Geophys. Res. Lett. 48.

Andrew, R., Guan, H., Batelaan, O., 2017. Estimation of GRACE water storage components by temporal decomposition. J. Hydrol. 552, 341–350.

Atlas, H., 2013. Hydro Atlas of United Arab Emirates. United Arab Emirates University.

Beaudoing, H., Rodell, M., 2020a. GLDAS Noah Land Surface Model L4 Monthly 1.0 x 1.0 Degree V2.1. Goddard Earth Sciences Data and Information Services Center (GES DISC).

Beaudoing, H., Rodell, M., 2020b. GLDAS VIC Land Surface Model L4 Monthly 1.0 x 1.0 Degree V2.1. Goddard Earth Sciences Data and Information Services Center (GES DISC).

Bettadpur, S., 2018. Gravity Recovery and Climate Experiment UTCSR Level-2 Processing Standards Document. Center for Space Research, The University of Texas at Austin.

Bhanja, S., Mukherjee, A., Saha, D., Velicogna, I., Famiglietti, J., 2016. Validation of GRACE based groundwater storage anomaly using in-situ groundwater level measurements in India. J. Hydrol. 543 (Part B), 729–738.

Bhanja, S.N., Rodell, M., Li, B., Saha, D., Mukherjee, A., 2017. Spatio-temporal variability of groundwater storage in India. J. Hydrol. 544, 428–437.

Bhanja, S.N., Zhang, X., Wang, J., 2018. Estimating long-term groundwater storage and its controlling factors in Alberta, Canada. Hydrol. Earth Syst. Sci. 22, 6241–6255.

Bi, H., Ma, J., Zheng, W., Zeng, J., 2016. Comparison of soil moisture in GLDAS model simulations and in situ observations over the tibetan plateau. Journal of Geophysical Research: Atmospheres 121, 2658–2678.

Biancamaria, S., Mballo, M., Le Moigne, P., Sánchez Pérez, J.M., Espitalier-Noël, G., Grusson, Y., Cakir, R., Häfliger, V., Barathieu, F., Trasmonte, M., Boone, A., Martin, E., Sauvage, S., 2019. Total water storage variability from GRACE mission and hydrological models for a 50,000 km2 temperate watershed: the Garonne River basin (France). J. Hydrol. Region. Stud. 24, 100609.

Bonsor, H.C., Shamsudduha, M., Marchant, B.P., Macdonald, A.M., Taylor, R.G., 2018. Seasonal and decadal groundwater changes in african sedimentary aquifers estimated using GRACE products and LSMs. Remote Sens. 10.

Brookfield, A.E., Hill, M.C., Rodell, M., Loomis, B.D., Stotler, R.L., Porter, M.E., Bohling, G.C., 2018. In situ and GRACE-based groundwater observations: similarities, discrepancies, and evaluation in the High Plains aquifer in Kansas. Water Resour. Res. 54, 8034–8044.

Chambers, D., 2006. Evaluation of new GRACE time-variable gravity data over the ocean. Geophys. Res. Lett. 331.

Chen, J.L., Wilson, C.R., Tapley, B.D., Scanlon, B., Güntner, A., 2016. Long-term groundwater storage change in Victoria, Australia from satellite gravity and in situ observations. Glob. Planet. Chang. 139, 56–65.

Cheng, M., Ries, J., 2019. GRACE Technical Note. 11.

Condon, L.E., Maxwell, R.M., 2015. Evaluating the relationship between topography and groundwater using outputs from a continental-scale integrated hydrology model. Water Resour. Res. 51, 6602–6621.

Cooley, S., Landerer, F., 2019. GRACE L-3 product user handbook. Jet Propulsion Laboratory California Institute of Technology.

Davijani, M., Banihabib, M.E., Nadjafzadeh Anvar, A., Hashemi, S.R., 2016. Multi-objective optimization model for the allocation of water resources in arid regions based on the maximization of socioeconomic efficiency. Water Resour. Manag. 30, 927–946.

Delhomme, J.P., 1978. Kriging in the hydrosciences. Adv. Water Resour. 1, 251–266.

Dennehy, K.F., Reilly, T.E., Cunningham, W.L., 2015. Groundwater availability in the United States: the value of quantitative regional assessments. Hydrogeol. J. 23, 16291632.

Dewandel, B., Gandolfi, J.M., de Condappa, D., Ahmed, S., 2008. An efficient methodology for estimating irrigation return flow coefficients of irrigated crops at watershed and seasonal scale. Hydrol. Process. 22, 1700–1712.

EAD, 2018. Groundwater Atlas of Abu Dhabi Emirate. Environment Agency of Abu Dhabi, UAE.

Ebrahimi, H., Ghazavi, R., Karimi, H., 2016. Estimation of groundwater recharge from the rainfall and irrigation in an arid environment using inverse modeling approach and RS. Water Resour. Manag. 30, 1939–1951.

Eggleston, M., Imes, Kress, Woodward, A.B., 2018. Hydrogeologic Framework and Simulation of Predevelopment Groundwater Flow, Eastern Abu Dhabi Emirate, United Arab Emirates. U.S. Geological Servey.

Fallatah, O.A., 2020. Groundwater quality patterns and spatiotemporal change in depletion in the regions of the Arabian Shield and Arabian Shelf. Arabian J. Sci. Eng. 45, 341–350.

Fallatah, O.A., Ahmed, M., Save, H., Akanda, A.S., 2017. Quantifying temporal variations in water resources of a vulnerable middle eastern transboundary aquifer system. Hydrol. Process. 31, 4081–4091.

Farr, T.G., Rosen, P.A., Caro, E., Crippen, R., Duren, R., Hensley, S., Kobrick, M., Paller, M., Rodriguez, E., Roth, L., Seal, D., Shaffer, S., Shimada, J., Umland, J., Werner, M., Oskin, M., Burbank, D., Alsdorf, D., 2007. The shuttle radar topography Mission. Rev. Geophys. 45.

Flechtner, F., Dobslaw, H., Fagiolini, E., 2015. AOD1B product description document for product release 05. http://www-app2.gfz-potsdam.de/pb1/op/grace/results/grav/AOD1B_20151214.pdf.

Fragaszy, S.R., McDonnell, 2016. Oasis at a Crossroads: Agriculture and Groundwater in Liwa, United Arab Emirates. International Water Management Institute.

Fu, G., Crosbie, R.S., Barron, O., Charles, S.P., Dawes, W., Shi, X., van Niel, T., Li, C., 2019. Attributing variations of temporal and spatial groundwater recharge: a statistical analysis of climatic and non-climatic factors. J. Hydrol. 568, 816–834.

Gent, P.R., Danabasoglu, G., Donner, L.J., Holland, M.M., Hunke, E.C., Jayne, S.R., Lawrence, D.M., Neale, R.B., Rasch, P.J., Vertenstein, M., Worley, P.H., Yang, Z.-L., Zhang, M., 2011. The community climate system model version 4. J. Clim. 24, 4973–4991.

Ghebreyesus, D.T., Temimi, M., Fares, A., Bayabil, H.K., 2016. A multi-satellite approach for water storage monitoring in an arid watershed. Geosciences 6, 33.

Ghorbal, A., Kallel, A., Ksibi, M., Dhia, H.B., Khélifi, N., 2021. Developing new approaches and strategies to promote sustainability and environmental integration in the Mediterranean region. Environ. Sci. Pollut. Res. Int. 28, 46414–46422.

Gido, N.A.A., Amin, H., Bagherbandi, M., Nilfouroushan, F., 2020. Satellite monitoring of mass changes and ground subsidence in Sudan's oil fields using GRACE and Sentinel-1 data. Remote Sens. 12, 1792.

Gonzalez, R., Ouarda, T., Marpu, P., Allam, M., Eltahir, E., Pearson, S., 2016. Water budget analysis in arid regions, application to the United Arab Emirates. Water 8.

Hachborn, E., Berg, A., Levison, J., Ambadan, J.T., 2017. Sensitivity of GRACE-derived estimates of groundwater-level changes in southern Ontario, Canada. Hydrogeol. J. 25, 2391–2402.

Hagström, E.L., Lyles, C., Pattanayek, M., Deshields, B., Berkman, M.P., 2016. Produced Water—Emerging challenges, risks, and opportunities. Environmental Claims Journal 28, 122–139.

Hamed, K.H., 2008. Trend detection in hydrologic data: the Mann Kendall trend test under the scaling hypothesis. J. Hydrol. 349, 350–363.

Han, D., Currell, M.J., Cao, G., Hall, B., 2017. Alterations to groundwater recharge due to anthropogenic landscape change. J. Hydrol. 554, 545–557.

Hu, Z., Zhou, Q., Chen, X., Chen, D., Li, J., Guo, M., Yin, G., Duan, Z., 2019. Groundwater depletion estimated from GRACE: a challenge of sustainable development in an arid region of Central Asia. Remote Sens. 11, 1908.

Hubbert, M.K., 1957. Darcy's law and the field equations of the flow of underground fluids. Int. Assoc. Sci. Hydrol. Bull. 2, 23–59.

Hussein, K.A., Alsumaiti, T.S., Ghebreyesus, D.T., Sharif, H.O., Abdalati, W., 2021. High-resolution spatiotemporal trend analysis of precipitation using satellite-based products over the United Arab Emirates. Water 13.

Imes, J.L., Wood, W.W., 2007. Solute and isotope constraint of groundwater recharge simulation in an arid environment, Abu Dhabi emirate, United Arab Emirates. Hydrogeol. J. 15, 1307–1315.

IWACO, 1986. Ground water study. Drilling of Deep Water Wells at Various locations in the UAE. Ministry of Energy and Infrastructure, Dubai, UAE.

Izady, A., Abdalla, O., Joodavi, A., Chen, M., 2017. Groundwater modeling and sustainability of a transboundary hardrock-alluvium aquifer in North Oman Mountains. Water 9.

Jafari, H., Sudegi, A., Bagheri, R., 2019. Contribution of rainfall and agricultural returns to groundwater recharge in arid areas. J. Hydrol. 575, 1230–1238.

Jasechko, S., Perrone, D., 2021. Global groundwater wells at risk of running dry. Science 372, 418–421.

Kaliraj, S., Chandrasekar, N., Magesh, N.S., 2013. Identification of potential groundwater recharge zones in vaigai upper basin, Tamil Nadu, using GIS-based analytical hierarchical process (AHP) technique. Arab. J. Geosci. 7, 1385–1401.

Kendall, M.G., 1955. Rank Correlation Methods. 2nd ed. .

Komuscu, A.U., 2017. Long-term mean monthly temperatures trends of the United Arab Emirates. Int. Journal of Global Warming 11, 1–22.

Landerer, F.W., Swenson, S.C., 2012. Accuracy of scaled GRACE terrestrial water storage estimates. Water Resour. Res. 48.

Lavalin INC, G.A.D., 1980. Report on the Discoveryof Submarine Springs Using Infrared Thermal Imagery. Internal Report Ministry of Agriculture and Fisheries, Dubai, UAE.

Lawrence, D.M., Oleson, K.W., Flanner, M.G., Thornton, P.E., Swenson, S.C., Lawrence, P.J., Zeng, X., Yang, Z.-L., Levis, S., Sakaguchi, K., Bonan, G.B., Slater, A.G., 2011. Parameterization improvements and functional and structural advances in version 4 of the community land model. J. Adv. Model. Earth Syst. 3.

Lezzaik, K., Milewski, A., 2018. A quantitative assessment of groundwater resources in the Middle East and North Africa region. Hydrogeol. J. 26, 251–266.

Li, B., Rodell, M., Kumar, S., Beaudoing, H.K., Getirana, A., Zaitchik, B.F., Goncalves, L.G., Cossetin, C., Bhanja, S., Mukherjee, A., Tian, S., Tangdamrongsub, N., Long, D., Nanteza, J., Lee, J., Policelli, F., Goni, I.B., Daira, D., Bila, M., Lannoy, G., Mocko, D., Steele-Dunne, S.C., Save, H., Bettadpur, S., 2019. Global GRACE data assimilation for groundwater and drought monitoring: advances and challenges. Water Resour. Res. 55, 7564–7586.

Li, B., Beaudoing, H., Rodell, M., 2020. GLDAS Catchment Land Surface Model L4 Monthly 1.0 x 1.0 Degree V2.1. Goddard Earth Sciences Data and Information Services Center (GES DISC).

Liesch, T., Ohmer, M., 2016. Comparison of GRACE data and groundwater levels for the assessment of groundwater depletion in Jordan. Hydrogeol. J. 24, 1547–1563.

Lin, M., Biswas, A., Bennett, E.M., 2019. Identifying hotspots and representative monitoring area of groundwater changes with time stability analysis. Sci. Total Environ. 667, 419–426.

Long, D., Chen, X., Scanlon, B.R., Wada, Y., Hong, Y., Singh, V.P., Chen, Y., Wang, C., Han, Z., Yang, W., 2016. Have GRACE satellites overestimated groundwater depletion in the Northwest India Aquifer? Sci. Rep. 6, 24398.

Madani, K., Aghakouchak, A., Mirchi, A., 2016. Iran's socio-economic drought: challenges of a water-bankrupt nation. Iran. Stud. 49, 997–1016.

Mann, H.B., 1945. Nonparametric tests against trend. Econometrica 13, 245–259.

Margat, J., van der Gun, J., 2013. Groundwater Around the World: A Geographic Synopsis. Crc Press.

Meinzer, O.E., 1923. The Occurrence of Ground Water in the United States, With a Discussion of Principles. Water Supply Paper. Washington, DC.

MOEW, IAEA, 2005. Assessment of Groundwater Recharge in Wadi Al Wurryah, Al Taween, and Al Bih Using Environmental Isotopes.

Mohamed, A., Abdelrahman, K.A.A., 2022. Application of time-variable gravity to groundwater storage fluctuations in Saudi Arabia. Front. Earth Sci. 10.

Moore, S., Fisher, J.B., 2012. Challenges and opportunities in GRACE-based groundwater storage assessment and management: an example from Yemen. Water Resour. Manag. 26, 1425–1453.

Naghedifar, S.M., Ziaei, A.N., Ansari, H., 2018. Simulation of irrigation return flow from a triticale farm under sprinkler and furrow irrigation systems using experimental data: a case study in arid region. Agric. Water Manag. 210, 185–197.

Nash, J.E., Sutcliffe, J.V., 1970. River flow forecasting through conceptual models part I — a discussion of principles. J. Hydrol. 10, 282–290.

NCMS, 2021. National Center for Meteorology and Seismology. Abu Dhabi, United Arab Emirates.

NDC, USGS, 1996. USGS. Groundwater Research Project. National Drilling Company and USGS, Al Ain, Abu Dhabi, United Arab Emirates.

Neves, M.C., Nunes, L.M., Monteiro, J.P., 2020. Evaluation of GRACE data for water resource management in Iberia: a case study of groundwater storage monitoring in the Algarve region. J. Hydrol. Region. Stud. 32, 100734.

Niranjan Kumar, N., Ouarda, T.B.M.J., 2014. Precipitation variability over UAE and global SST teleconnections. J. Geophys. Res. Atmos. 119, 10313–10322.

Osterkamp, L.A.M., 1995. Techniques of groundwater-recharge estimates in arid/semi-arid areas, with examples from Abu Dhabi. J. Arid Environ. 349–369.

Osterkamp, W.R., Lane, L.J., Menges, C.M., 1995. Techniques of ground-water recharge estimates in arid/semi-arid areas, with examples from Abu Dhabi. J. Arid Environ. 31, 349–369.

Ouma, Y.O., Aballa, D.O., Marinda, D.O., Tateishi, R., Hahn, M., 2015. Use of GRACE timevariable data and GLDAS-LSM for estimating groundwater storage variability at small basin scales: a case study of the Nzoia River basin. Int. J. Remote Sens. 36, 5707–5736.

Panda, B., Sabarathinam, C., Nagappan, G., Rajendiran, T., Kamaraj, P., 2021. Multiple thematic spatial integration technique to identify the groundwater recharge potential zones—a case study along the Courtallam Region, Tamil Nadu, India. Arab. J. Geosci. 13.

Peltier, R., Donald, F.W.A., Drummond, R., 2018. Comment on "an assessment of the ICE-6G_C (VM5a) glacial isostatic adjustment model" by Purcell et al. Journal of Geophysical Research: Solid Earth 123, 2019–2028.

PIK, 2007. Development of Functional Irrigation Types for Improved Global Crop Modelling. Potsdam Institute for Climate Impact Research (PIK), Potsdam.

Rahimzadegan, M., Entezari, S.A., 2019. Performance of the gravity recovery and climate experiment (GRACE) method in monitoring groundwater-level changes in local-scale study regions within Iran. Hydrogeol. J. 27, 2497–2509.

Ramjeawon, M., Demlie, M., Toucher, M., 2022. Analyses of groundwater storage change using GRACE satellite data in the Usutu-Mhlatuze drainage region, North-Eastern South Africa. J. Hydrol. Region. Stud. 42, 101118.

Rateb, A., Scanlon, B.R., Pool, D.R., Sun, A., Zhang, Z., Chen, J., Clark, B., Faunt, C.C., Haugh, C.J., Hill, M., Hobza, C., McGuire, V.L., Reitz, M., Müller Schmied, H., Sutanudjaja, E.H., Swenson, S., Wiese, D., Xia, Y., Zell, W., 2020. Comparison of groundwater storage

changes from GRACE satellites with monitoring and modeling of major U.S. aquifers. Water Resources Research 56, e2020WR027556.

Richey, A.S., Thomas, B.F., Lo, M.-H., Reager, J.T., Famiglietti, J.S., Voss, K., Swenson, S., Rodell, M., 2015. Quantifying renewable groundwater stress with GRACE. Water Resour. Res. 51, 5217–5238.

Rodell, M., Famiglietti, J.S., 2001. An analysis of terrestrial water storage variations in Illinois with implications for the gravity recovery and climate experiment (GRACE). Water Resour. Res. 37, 1327–1339.

Rodell, M., Houser, P.R., Jambor, U., Gottschalck, J., Mitchell, K., Meng, C.J., Arsenault, K., Cosgrove, B., Radakovich, J., Bosilovich, M., Entin, J.K., Walker, J.P., Lohmann, D., Toll, D., 2004. The global land data assimilation system. Bull. Am. Meteorol. Soc. 85, 381–394.

Rodell, M., Beaudoing, H.K., L'Ecuyer, T.S., Olson, W.S., Famiglietti, J.S., Houser, P.R., Adler, R., Bosilovich, M.G., Clayson, C.A., Chambers, D., Clark, E., Fetzer, E.J., Gao, X., Gu, G., Hilburn, K., Huffman, G.J., Lettenmaier, D.P., Liu, W.T., Robertson, F.R., Schlosser, C.A., Sheffield, J., Wood, E.F., 2015. The observed state of the water cycle in the early twenty-first century. J. Clim. 28, 8289–8318.

Rodell, M., Famiglietti, J.S., Wiese, D.N., Reager, J.T., Beaudoing, H.K., Landerer, F.W., Lo, M.H., 2018. Emerging trends in global freshwater availability. Nature 557, 651.

Saber, M., Alhinai, S., Al Barwani, A., Al-Saidi, A., Kantoush, S.A., Habib, E., Borrok, D.M., 2017. Satellite-Based Estimates of Groundwater Storage Changes at the Najd Aquifers in Oman. In: Abdalla, O., Kacimov, A., Chen, M., Al-Maktoumi, A., Al-Hosni, T., Clark, I. (Eds.), Water Resources in Arid Areas: The Way Forward. Springer International Publishing, Cham, pp. 155–169.

Sathish, S., Mohamed, M., Klammler, H., 2018. Regional groundwater flow model for Abu Dhabi emirate: scenario-based investigation. Environ. Earth Sci. 77, 409.

SCAD, 2020. Statistics Center Abu Dhabi.

Scanlon, B.R., Longuevergne, L., Long, D., 2012. Ground referencing GRACE satellite estimates of groundwater storage changes in the California Central Valley, USA. Water Resour. Res. 48.

Scanlon, B.R., Zhang, Z., Save, H., Wiese, D.N., Landerer, F.W., Long, D., Longuevergne, L., Chen, J., 2016. Global evaluation of new GRACE mascon products for hydrologic applications. Water Resour. Res. 52, 9412–9429.

Selvam, S., Magesh, N.S., Chidambaram, S., Rajamanickam, M., Sashikkumar, M.C., 2014. A GIS based identification of groundwater recharge potential zones using RS and IF technique: a case study in Ottapidaram Taluk, Tuticorin District, Tamil Nadu. Environ. Earth Sci. 73, 3785–3799.

Sen, P.K., 1968. Estimates of the regression coefficient based on Kendall's Tau. Journal of the American Statistical Association 63, 1379–1389.

Seo, K.W., Wilson, C.R., Famiglietti, J.S., Chen, J.L., Rodell, M., 2006. Terrestrial water mass load changes from gravity recovery and climate experiment (GRACE). Water Resour. Res. 42.

Seraphin, P., Gonçalvès, J., Hamelin, B., Stieglitz, T., Deschamps, P., 2022. Influence of intensive agriculture and geological heterogeneity on the recharge of an arid aquifer system (Saq-Ram, Arabian Peninsula). EGUsphere 2022, 1–22.

Shamsudduha, M., Taylor, R.G., 2020. Groundwater storage dynamics in the world's large aquifer systems from GRACE: uncertainty and role of extreme precipitation. Earth Syst. Dynam. 11, 755–774.

Shamsudduha, M., Taylor, R.G., Longuevergne, L., 2012. Monitoring groundwater storage changes in the highly seasonal humid tropics: validation of GRACE measurements in the Bengal Basin. Water Resour. Res. 48.

Sherif, M., Sefelnasr, A., Ebraheem, A.A., Al Mulla, M., Alzaabi, M., Alghafli, K., 2021. Spatial and temporal changes of groundwater storage in the quaternary aquifer, UAE. Water 13.

Sherif, M.M., Ebraheem, A.M., Al Mulla, M.M., Shetty, A.V., 2018. New system for the assessment of annual groundwater recharge from rainfall in the United Arab Emirates. Environ. Earth Sci. 77 (11).

Shi, J.X., Wild, M., Lettenmaier, D., 2010. Surface radiative fluxes over the pan-Arctic land region: variability and trends. J. Geophys. Res. 115.

Shi, J.X., Vaze, J., Crosbie, R., 2015. The Controlling Factors in the Daily and Monthly Groundwater Recharge Estimation Using the Water Table Fluctuation Method.

Strassberg, G., Scanlon, B.R., Rodell, M., 2007. Comparison of seasonal terrestrial water storage variations from GRACE with groundwater-level measurements from the High Plains aquifer (USA). Geophys. Res. Lett. 34.

Sun, A.Y., Green, R., Rodell, M., Swenson, S., 2010. Inferring aquifer storage parameters using satellite and in situ measurements: estimation under uncertainty. Geophys. Res. Lett. 37.

Sun, Y., Riva, R., Ditmar, P., 2016. Optimizing estimates of annual variations and trends in geocenter motion and J2 from a combination of GRACE data and geophysical models. Journal of Geophysical Research: Solid Earth 121, 8352–8370.

Swenson, S., Wahr, J., 2006. Post-processing removal of correlated errors in GRACE data. Geophys. Res. Lett. 33.

Swenson, S., Yeh, P.J.F., Wahr, J., Famiglietti, J., 2006. A comparison of terrestrial water storage variations from GRACE with in situ measurements from Illinois. Geophys. Res. Lett. 33, L16401.

Tapley, B., Bettadpur, S., Ries John, C., Thompson Paul, F., Watkins Michael, M., 2004. GRACE measurements of mass variability in the earth system. Science 305, 503–505.

Taylor, R., Aureli, A., Allen, D., Banks, D., Villholth, K., Stigter, T., Shamsudduha, M., Akhurst, M., Hartog, N., Green, T., Vystavna, Y., 2022. Chapter 7: Groundwater, Aquifers and Climate Change.

Todd, D.K., Mays, L.W., 2005. Groundwater Hydrology, Hoboken. John Wiley & Sons Inc.

Walker, D., Parkin, G., Schmitter, P., Gowing, J., Tilahun, S.A., Haile, A.T., Yimam, A.Y., 2019. Insights from a multi-method recharge estimation comparison study. Ground Water 57, 245–258.

Wang, S., Liu, H., Yu, Y., Zhao, W., Yang, Q., Liu, J., 2020. Evaluation of groundwater sustainability in the arid hexi corridor of northwestern China, using GRACE, GLDAS and measured groundwater data products. Sci. Total Environ. 705, 135829.

Watkins, M.M., Wiese, D.N., Yuan, D.-N., Boening, C., Landerer, F.W., 2015. Improved methods for observing Earth's time variable mass distribution with GRACE using spherical cap mascons. Journal of Geophysical Research: Solid Earth 120, 2648–2671.

Wehbe, Y., Temimi, M., 2021. A remote sensing-based assessment of water resources in the arabian peninsula. Remote Sens. 13, 247.

Wehbe, Y., Temimi, M., Ghebreyesus, D.T., Milewski, A., Norouzi, H., Ibrahim, E., 2018. Consistency of precipitation products over the arabian peninsula and interactions with soil moisture and water storage. Hydrol. Sci. J. 63, 408–425.

White, E.K., Peterson, T.J., Costelloe, J., Western, A.W., Carrara, E., 2016. Can we manage groundwater? A method to determine the quantitative testability of groundwater management plans. Water Resour. Res. 52, 4863–4882.

Wiese, D.N., Landerer, F.W., Watkins, M.M., 2016. Quantifying and reducing leakage errors in the JPL RL05M GRACE mascon solution. Water Resour. Res. 52, 7490–7502.

Wiese, D.N., Yuan, D.N., Boening, C., Landerer, F.W., Watkins, M.M., 2018. JPL GRACE Mascon Ocean, Ice, and Hydrology Equivalent Water Height Release 06 Coastal Resolution Improvement (CRI) Filtered Version 1.0. Ver. 1.0. PO. DAAC, CA, USA.

Woodward, D.G., Menges, C.M., 1992. Neotectonic thrust faulting along the western flank of the Oman Mountains, northeastern Abu Dhabi, Pan 2. Hydrogeologic Implications. 73.

World-Bank, 2017. Beyond Scarcity: Water Security in the Middle East and North Africa. MENA Development Series. World Bank, Washingron, DC.

Yakirevich, A., Weisbrod, N., Kuznetsov, M., Rivera Villarreyes, C.A., Benavent, I., Chavez, A.M., Ferrando, D., 2013. Modeling the impact of solute recycling on groundwater salinization under irrigated lands: a study of the Alto Piura aquifer, Peru. J. Hydrol. 482, 25–39.

Yassin, M., Makkawi, M., Pradipta, A., Karami, G., Benaafi, M., 2019.. Spatial distribution and temporal variation of groundwater storage in Saudi Arabia. Space-based Observation Approach, p. 12547.

Yin, W., Li, T., Zheng, W., Han, S.-C., Hu, L., Tangdamrongsub, N., Šprlák, M., Zhiyong, H., 2020. Improving regional groundwater storage estimates from GRACE and global hydrological models over Tasmania, Australia. Hydrogeol. J. 28, 1–17.

Yu, Y., Pi, Y., Yu, X., Ta, Z., Sun, L., Disse, M., Zeng, F., Li, Y., Chen, X., Yu, R., 2019. Climate change, water resources and sustainable development in the arid and semi-arid lands of Central Asia in the past 30 years. J. Arid Land 11, 1–14.